Award Number: W81XWH-12-0255

TITLE: Genetic Networks Activated by Blast Injury to the Eye

PRINCIPAL INVESTIGATOR: Eldon E. Geisert

CONTRACTING ORGANIZATION: Emory University
Atlanta, GA 30322

REPORT DATE: August 2015

TYPE OF REPORT: Annual

PREPARED FOR: U.S. Army Medical Research and Materiel Command
Fort Detrick, Maryland 21702-5012

DISTRIBUTION STATEMENT: Approved for Public Release;
Distribution Unlimited

The views, opinions and/or findings contained in this report are those of the author(s) and should not be construed as an official Department of the Army position, policy or decision unless so designated by other documentation.

REPORT DOCUMENTATION PAGE

Form Approved
OMB No. 0704-0188

1. REPORT DATE	2. REPORT TYPE	3. DATES COVERED
August 2015	Annual	July 15, 2014 - July 14,2015

4. TITLE AND SUBTITLE
Genetic Networks Activated by Blast Injury to the Eye

Sa. CONTRACT NUMBER

Sb. GRANT NUMBER
W81XWH-12-1-0255

Sc. PROGRAM ELEMENT NUMBER

6. AUTHOR(S)
Eldon E. Geisert

E-Mail: egeiser@emory.edu

Sd. PROJECT NUMBER

Se. TASK NUMBER

Sf. WORK UNIT NUMBER

7. PERFORMING ORGANIZATION NAME(S) AND ADDRESS(ES)
Emory University
Atlanta, GA 30322

8. PERFORMING ORGANIZATION REPORT

9. SPONSORING / MONITORING AGENCY NAME(S) AND ADDRESS(ES)
U.S. Army Medical Research and Materiel Command
Fort Detrick, Maryland 21702-5012

10. SPONSOR/MONITOR'S ACRONYM(S)

11. SPONSOR/MONITOR'S REPORT NUMBER(S)

12. DISTRIBUTION / AVAILABILITY STATEMENT
Approved for Public Release; Distribution Unlimited

13. SUPPLEMENTARY NOTES

14. ABSTRACT

The present grant proposes to look at the effects of blast on the eye of the mouse looking at phenotypic changes in the eye and in the changes in gene expression following a 50psi blast. We are using these data to define biomarkers to predict the severity of the injury and to predict eventual outcomes. We have examined the phenotypic changes in the eye in the BXD strains before and 5 days after a 50psi blast and have observed no strain specific change in either the cornea or the IOP. We have completed the normal retina database containing 222 microarrays from 58 strains of mice. We have also prepared the manuscript describing the database and submitted it to Molecular Vision for publication. The database and annotation are complete and will be released to the public upon the acceptance of the manuscript. We have collected 76 retinas from 19 strains 5 days after a 50psi blast. These retinas are being held for a batch RNA isolation and microarray run. Microarrays were run on an additional 27 strains. Next year we will complete the dataset by adding 84 retinas from 21 BXD strains. We have taken a preliminary examination of the blast dataset and found that Soxl 1 is a relatively good marker for injured retinal ganglion cells. These results are presented in a paper currently under revision for publication in Molecular Vision.

15. SUBJECT TERMS
Nothing Listed

16. SECURITY CLASSIFICATION OF:			17. LIMITATION OF ABSTRACT	18. NUMBER OF PAGES	19a. NAME OF RESPONSIBLE PERSON
a. REPORT	b. ABSTRACT	c. THIS PAGE			USAMRMC
Unclassified	Unclassified	Unclassified	Unclassified	51	19b. TELEPHONE NUMBER *(include area code)*

Table of Contents

1 INTRODUCTION

In a collaboration with Dr. Tonia Rex we developed a mouse model of blast injury to the eye, which accurately mimics the traumatic blast injury increasingly suffered by warriors under current battlefield conditions (Hines-Beard et al., 2012). Using this mouse model in combination with a powerful combination of systems biology, microarray analysis, expression genetics, and bioinformatics, we are defining the genetic networks activated by the ocular blast injury. At the heart of our approach is a genetic reference panel of mice, the unique resource of BXD recombinant inbred (RI) strain set. The set of RI strains was produced from a genetic cross between the C57BU6J mouse and the DBA/2J mouse. Using 60 BXD strains provides a new and powerful method to defining elements in the genome regulating the response of the eye to blast injury. This allows us to generate specific, testable hypotheses to define the pathways that regulate the response of the eye to blast injury and reactive responses in the retina. As more diverse gene expression data sets become available, comparison of gene expression and regulation in different biological contexts will help identify the regulatory elements controlling the injury response of the eye and the retina. We are currently identifying genetic networks activated by blast injury and the genomic regions controling these networks. We are also identifying markers for retinal injury and potential targets for intervention.

2 KEYWORDS

Mouse Genomics, Blast Injury, Eye, Retina, Gene Expression, Microarray

3 ACCOMPLISHMENTS

Maior Goals:

Task 1) Quantify the strain-to-strain differences in the severity of blast-induced ocular pathologies, using a set of 60 BXD RI mouse strains and map the genomic loci that regulate the response of the eye to blast injury. In this Task we were measuring intraocular pressure (IOP), central corneal thickness (CCT) and visual acuity.

Task 2) Define the genetic networks activated by blast injury in the eye and in the retina, using transcriptome-wide profiling across the BXD RI strain set. We are using the Affymetrix GeneChip Gene 2.0 ST Mouse Array to characterize the changes occurring following a blast injury to the eye in 60 BXD strains. There were several major benefits to using the new Affymetrix array. Specifically, there are probes for 7,000 non-coding RNAs (RNA that is not converted to protein but does affect the functioning of the cell). We are now finding out that many of these non-coding RNAs play extremely important roles in the body. Within these 7,000 probes, 588 encode microRNAs (small RNAs that regulate protein expression). We are creating an entire normal retina dataset using the Affymetrix GeneChip Gene 2.0 Mouse Array and comparing this data set to a dataset from retinas 5 days after a 50psi blast injury to the eye.

Task 3) Define biomarkers that can predict the severity of injury and eventual outcomes.

This portion of our study was to begin in the latter years of the grant (Months 40 to 48). We are using this to characterize the 50-psi blast injury in advance of resuming the blast microarray study on the BXD RI strain set. Immunostaining sections of retina revealed that SOX11 was upregulated in the neurons of the inner retina following blast. SOX11 labeled cells in the ganglion cell layer and the inner nuclear layer. In the ganglion cell layer SOX11 labeled a majority of the cells, indicating that it was labeling most ganglion cells and displaced amacrine cells. Once the datasets are fully implemented, we will be able to accurately define the changes occurring within the injured retina.

Accomplishments Under These Goals:

Task1:

At the present time we have measured IOP and central corneal thickness on 33 strains of mice before and after a 50psi blast injury to the eye. At the present time there are 117 animals total in the dataset. When we run a student t test on the data there was no significant difference in CCT or IOP before and after blast in the control eyes. This is expected. We also did not see a significant difference in either CCT or IOP 5 days after a 50psi blast to the experimental eye. This is unexpected. We intend to continue measuring CCT and IOP measurements for the next quarter.

Task 2.

A) We have completed the construction of the DoD CDMRP Normal Retinal Dataset. Using the Affymetrix Mouse Gene 2.0 ST array, to interrogate all exons of traditional protein coding genes, non-coding RNAs and microRNAs. These data are presented in a highly interactive database within the GeneNetwork website. In the Normal Retina Database, we quantified mRNA levels of the transqriptome from retinas using the Affymetrix Mouse Gene 2.0 ST array. The Normal Retina Database consists of gene expression data from male and female mice. The dataset includes a total of 55 BXD RI strains, the parental strains (C57Bl/6J and DBA/2J), and a reciprocal cross. In combination with GeneNetwork, the DoD (Department of Defense) CDMRP (Congressionally Directed Medical Research Programs) Normal Retina Database provides a large resource for mapping, graphing, analyzing, and testing complex genetic networks. Protein-coding and non-coding RNAs can be used to map quantitative trait loci (QTLs) that contribute to expression differences among the BXD strains and to establish links between classical ocular phenotypes associated with differences in genomic sequence. With this resource we are able to extract transcriptome signatures for retinal cells and to define genetic networks associated with the maintenance of the normal retina. Ultimately, we will use this database to define changes occurring following blast injury to the retina. The DoD CDMRP Normal Retina Database uses the Affymetrix MouseGene 2.0 ST Array (May 15 2015). The RMA analysis and scaling was conducted by Arthur Centeno. This data set consists of 55 BXD strains, C57BU6J, DBA/2J, an F1 cross between C57BU6J and DBA/2J. A total of 58 strains were quantified. There is a total of 222 microarrays. All of the data from each of the microarrays used in this dataset is publically available on GeneNetwork.org.

Mice were killed by rapid cervical dislocation. Retinas were removed immediately and placed in 1 ml of 160 U/ml Ribolock for 1 min at room temperature. The retinas were removed from the eye and placed in Hank's Balanced Salt solution with RiboLock in 50µ1 Ribolock (Thermo Scientific RiboLock RNase #E00381 40U/µI 2500U) and stored in -80°C. The RNA was isolated using a QiaCube. All RNA samples were checked for quality before running microarrays. The samples were analyzed using the Agilent 2100 Bioanalyzer. The RNA integrity values ranged from 7.0 to 10. Our goal was to obtain data for independent biological sample pools from both sexes for most lines of mice. The four batches of arrays included in this final data set collectively represent a reasonably well-balanced sample of males and females, in general without within-strain-by-sex replication.

The data is presented using the Affymetrix Mouse Gene 2.0 ST Array. These expression arrays have been designed with a median of 22 unique probes per transcript. Each unique probe is 25 bases in length, which means that the array measures a median of 550 bases per transcript. The arrays provide comprehensive transcriptome coverage with over 30,000 coding and non-coding transcripts. In addition there is coverage for over 600 microRNAs. For some arrays the RNA was pooled from two retinas and other arrays were run on a single retina. Dr. XiangDi Wang (UTHSC) and Rebecca King (Emory) were involved in the retinal extractions and isolation of RNA. Two different research cores ran the Affymetrix arrays: the Molecular Resource Center at UTHSC (Dr. William Taylor Director) and the Integrated Genomics Core at Emory University by Robert B. Isett (Dr. Michael E. Zwick, Director). In a separate set of experiments we tested a set of arrays from C57BU6J retinas run at each facility to determine if there were batch effects or other confounding differences in the results. We could not detect any significant difference in the arrays run at UTHSC or at Emory University. Thus, we have included both sets of data into the analysis.

Publication: Rebecca King, Lu Lu, Robert W. Williams and Eldon E. Geisert, (2015) Gene Expression and Genetic Networks in the Mouse Retina, Submitted to Molecular Vision (under review).

Task 3) We have identified a list of potential biomarkers for injury to the retinal ganglion cells. The best marker is SOX11 (manuscript being revised). We are using this to characterize the 50psi blast injury in advance of resuming the blast microarray study on the BXD RI strain set. Immunostaining sections of retina revealed that SOX11 was upregulated in the neurons of the inner retina following blast. SOX11 labeled cells in the ganglion cell layer and the inner nuclear layer. In the ganglion cell layer SOX11 labeled a majority of the cells, indicating that it was labeling most ganglion cells and displaced amacrine cells. Amacrine cells in the inner nuclear layer were also lightly labeled by SOX11. On immunoblots there was approximately a 2-fold increase in the intensity of the SOX11 band. The manuscript describing these results is currently being revised to respond to the editorial suggestions.

Publication: Felix L. Struebing, Steven G. Hart, Joseph M. Caron, XiangDi Wang and Eldon E. Geisert (2015) Upregulation of SOX11 in Retinal Ganglion Cells Following Injury. Molecular Vision (under revision prior to resubmission).

Training and Professional Development Opportunities:

Nothing to Report

Dissemination of Results:

Invited Talks:

2014 Genetic Network of Innate Immunity in the Retina: Relevance to CNS Injury and Disease Department of Molecular Physiology and Biophysics University of Iowa.

2014 Genetic Network of Innate Immunity in the Retina: Relevance to CNS Injury and Disease VA Atlanta GA.

ARVO Meeting:
Sidhu C, Lyuboslavsky P, Chrenek MA, Struebing FL, Sellers JT, Setterholm NA, McDonals FE, Boatright JH, Geisert EE, Iuvone PM: 'Traumatic Blast-Induced Closed Globe Injury Reduces Visual Function in Retinal Ganglion Cells of Thy1-CFP mice: Mitigation by a Small Molecule TrkB Activator'', The Association for Research in Vision and Ophthalmology (ARVO) annual meeting, Denver 2015.

Papers Submitted for Publication:
Rebecca King, Lu Lu, Robert W. Williams and Eldon E. Geisert, (2015) Gene Expression and Genetic Networks in the Mouse Retina, Submitted to Molecular Vision (under review).

Felix L. Struebing, Steven G. Hart, Joseph M. Caron, XiangDi Wang and Eldon E. Geisert (2015) Upregulation of SOX11 in Retinal Ganglion Cells Following Injury. Molecular Vision (under revision prior to resubmission).

Plans for Next Reporting Period to Accomplish the Goals:

1) Finish Beta testing and open the DoD CDMRP Normal Retina Database to the public in August 2015.

2) We will complete the DoD Blast Microarray Database. This will entail running several hundred microarrays along with the costs of analysis. We anticipate this to consume a significant amount of the remaining budget.

3) Prepare manuscript describing the Blast database.

4) Release the Blast database to the public.

4 IMPACT

Impact on the Development of the Principal Discipline of the Project:

Once the proposed studies are completed they will provide a comprehensive analysis of the molecular pathways activated in the retina by blast injury to the eye.

Impact on Other Disciplines:

When developing Biomarkers for retinal injury, our microarray dataset will provide a means to determine if any specific biomarker could have originated from the retinal injury itself.

Impact on Society Beyond Science and Technology:

Nothing to Report

5) Changes/Problems

Changes in Approach and Reasons for Change:
None

Actual or Anticipated Problems or Delays and Actions or Plans to Resolve Them:
None

Changes that had Significant Impact on Expenditures:
None

Significant Changes in the Use or Care of Human Subjects Vertebrate Animals Biohazards, or Select Agents:
None

6. PRODUCTS

Publications, conference papers, and presentations:

2014 Genetic Network of Innate Immunity in the Retina: Relevance to CNS Injury and Disease Department of Molecular Physiology and Biophysics University of Iowa.

2014 Genetic Network of Innate Immunity in the Retina: Relevance to CNS Injury and Disease VA Atlanta GA.

ARVO Meeting:
Sidhu C, Lyuboslavsky P, Chrenek MA, Struebing FL, Sellers JT, Setterholm NA, McDonals FE, Boatright JH, Geisert EE, Iuvone PM: "Traumatic Blast-Induced Closed Globe Injury Reduces Visual Function in Retinal Ganglion Cells of Thy1-CFP mice: Mitigation by a Small Molecule TrkB Activator", The Association for Research in Vision and Ophthalmology (ARVO) annual meeting, Denver 2015.

Papers Submitted for Publication:
Rebecca King, Lu Lu, Robert W. Williams and Eldon E. Geisert, (2015) Gene Expression and Genetic Networks in the Mouse Retina, Submitted to Molecular Vision (under review).

Felix L. Struebing, Steven G. Hart, Joseph M. Caron, XiangDi Wang and Eldon E. Geisert (2015) Upregulation of SOX11 in Retinal Ganglion Cells Following Injury. Molecular Vision (under revision prior to resubmission).

Website(s) or other Internet site(s):

The DoD CDMRP Retina Affy MoGene 2.0 ST Database and the DoD TATRC Retina Affy MoGene 2.0 ST Exon Level Database are hosted on GeneNetwork.org. This database will be open to the public in August 2015. These datasets describe gene expression in the normal retina of the BXD Strains. Both databases can be found under Mice, BXD, retina and then either DoD CDMRP Retina Affy MoGene 2.0 ST Database or DoD CDMRP Retina Affy MoGene 2.0 ST Exon Level Database.

Technologies or techniques:
None

Inventions, patent applications, and/or licenses:
None

Other products:
None

7.PARTICIPANTS & OTHER COLLABORATING ORGANIZATIONS

What individuals have worked on the project?

At Emory University (7/15/14 to present):

Becky King, Research Technician (50% effort)
Eldon E. Geisert, Principal Investigator (25% effort)

We have been collaborating with Dr. Mike Iuvone to construct and test a new blast gun. We are currently in the process of writing a manuscript describing the effects of a 50psi blast to the mouse eye.

Has there been a change in the other active support of the PD/PI(s) or senior/key personnel since the last reporting period?

No.

What other organizations have been involved as partners?
None

8. SPECIAL REPORTING REQUIREMENTS

None

9. APPENDICES

A) Preprint of the DoD CDMRP Normal Retina Database paper.

8) Preprint of the SOX11 (marker of retinal injury)_ paper.

Gene Expression and Genetic Networks in the Mouse Retina

Rebecca King,[1] Lu Lu, [2] Robert W. Williams, [2] and Eldon E. Geisert, [1]

[1]Department of Ophthalmology and Emory Eye Center, Emory University, Atlanta, GA 30322; [2]Department of Anatomy and Neurobiology and Center for Integrative and Translational Genomics, University of Tennessee Health Science Center, Memphis, TN 38163

Corresponding Author:
Eldon E. Geisert
Professor of Ophthalmology
Emory University
1365B Clifton Road NE
Atlanta GA 30322
email: egeiser@emory.edu
Phone: 404-778-4239

Abstract

Purpose: Differences in gene expression provide diverse retina phenotypes and may also contribute to susceptibility to injury and disease. The present study defines the transcriptome of the retina in the BXD RI strain set. Using the Affymetrix Mouse Gene 2.0 ST array, to interrogate all exons of traditional protein coding genes, non-coding RNAs and microRNAs. These data are presented in a highly interactive database within the GeneNetwork website.

Methods: In the Normal Retina Database, quantified mRNA levels of the transcriptome from retinas using the Affymetrix Mouse Gene 2.0 ST array. The Normal Retina Database consists of gene expression data from male and female mice. The dataset includes a total of 55 BXD RI strains, the parental strains (C57Bl/6J and DBA/2J), and a reciprocal cross.

Results: In combination with GeneNetwork, the DoD (Department of Defense)

CDMRP (Congressionally Directed Medical Research Programs) Normal Retina Database provides a large resource for mapping, graphing, analyzing, and testing complex genetic networks. Protein-coding and non-coding RNAs can be used to map quantitative trait loci (QTLs) that contribute to expression differences among the BXD strains and to establish links between classical ocular phenotypes associated with differences in genomic sequence. With this resource we are able to extract transcriptome signatures for retinal cells and to define genetic networks associated with the maintenance of the normal retina. Ultimately, we will use this database to define changes occurring following blast injury to the retina.

Conclusions: The high level of variation in mRNA levels found among BXD RI strains of mice make it possible to identify expression networks underlying differences in retina structure and function.

INTRODUCTION

Large-scale sequencing initiatives have led to a new era in understanding gene and genome functions [1-5]. There is now an acute need for powerful approaches to integrate and analyze massive omics data sets. For vision research there are many known single gene variants that cause vision loss, including retinitis pigmentosa [6-9], Usher's syndrome [10, 11] and some forms of glaucoma [12]. However, many ocular diseases have a complex genetic basis with multiple chromosomal loci contributing to differences in susceptibility and severity of disease. Two prominent examples are glaucoma [13-15] and age-related macular degeneration [16, 17]. In addition, the response of the eye and retina to trauma is driven by a host of different genes expressed in a large number of different cell types.

Until recently, it was extremely difficult to define the genetic and molecular basis of complex diseases or to adequately monitor the response of eye and retina to injury. We have usee a novel and powerful approach relying on systems biology and a mouse genetic reference panel, the BXD family of recombinant inbred (RI) strains. This resource is particularly well suited to define complex genetic networks that are also active in human diseases. This approach not only allows us to identify specific gene variants involved in the retinal disease and response to injury, but also allows us to place corresponding moelcular changes in a global contest in eye and retina.

Our initial efforts of our group explored the genetic diversity of the BXD family of strains to define genetic networks active in the eye (see data sets and refs [18]) and ([19]).

In this study we have created the new mouse retinal database that offers a more complete description of the mouse transcriptome. This resource uses the genetic covariance of expression across a panel of 55 BXD strains to identify cellular signatures and genetic networks within the mouse retina. The array we have used provides expression profiling at the exon level for 26,191 well-established annotated transcripts, as well as 9,049 non-coding RNAs including over 600 microRNAs. Using the bioinformatics tools located within GeneNetwork (genenetwork.org), we examine a cellular signature of RPE cells. We also have analyzed a genetic and molecular network involved in neuronal development and axon growth. In both of these examples we highlight the specific benefits of the new database with a special emphasis on microRNAs, non-coding RNAs and the exon level data available with the Affymetrix MouseGene 2.0 ST array.

MATERIALS and METHODS

The DoD (Department of Defense) CDMRP (Congressionally Directed Medical Research Programs) Normal Retina Database uses the Affymetrix MouseGene 2.0 ST Array (May 15 2015). The RMA analysis and scaling was conducted by Arthur Centeno. This data set consists of 55 BXD strains, C57BL/6J, DBA/2J, an F1 cross between C57BL/6J and DBA/2J. A total of 58 strains were quantified. There is a total of 222 microarrays. All of the data from each of the microarrays used in this dataset is publically available on GeneNetwork.org.

This is RMA expression data that has been normalized using what we call a 2*z*+8 scale, but without special correction for batch effects. The data for each strain was computed as the mean of four samples per strain. Expression values on a log2 scale range from 3.81 to 14.25 (10.26 units), a nominal range of approximately 1,000-fold. After taking the log2 of the original non-logged expression estimates, we convert data within an array to a z-score. We then multiply the z-score by 2. Finally, we add 8 units to ensure that no values are negative. The result is a scale with a mean expression of the probes on the array of 8 units and a standard deviation of 2 units. A two-fold difference in expression is equivalent roughly to 1 unit on this scale. The lowest level of expression is 3.81 (*Olfr1186*) from DoD CDMRP (Normal Retina Database uses the Affymetrix MouseGene 2.0 ST Array (May 15 2015) The highest level of expression is Rhodopsin for *17462036* (Rho). Highest single value is about 14.25.

About the cases used to generate this set of data:
Almost all animals are young adults between 60 and 100 days of age. We measured expression in conventional inbred strains, BXD recombinant inbred (RI) strains, and reciprocal F1s between C57BL/6J and DBA/2J.

BXD strains:
The first 32 of these strains are from the Taylor series of BXD strains generated at the Jackson Laboratory by Benjamin A. Taylor. BXD1 through BXD32 were started in the late 1970s, whereas BXD33 through 42 were started in the 1990s. BXD43 and higher were bred by Lu Lu, Jeremy Peirce, Lee M. Silver, and Robert W. Williams starting in 1997 using B6D2 generation 10 advanced intercross progeny. This modified breeding protocol doubles the number of recombinations per BXD strain and improves mapping resolution [20]. All of the Taylor series of BXD strains and many of the new BXD strains are available from the Jackson Laboratory. Several strains were specifically excluded from the dataset. For the BXD43 and higher, the DBA/2J parent carried both the *Tyrp-1* mutation and the *Gpnmb* mutation and these two mutations produce pigment dispersion glaucoma. All of the mice carrying these two mutations were not included in the dataset: BXD53, BXD55, BXD62, BXD66, BXD68, BXD74, BXD77, BXD81, BXD88, BXD89, BXD95 and BXD98. In addition BXD24 was omitted, since it developed a spontaneous mutation, *rd16* (Cep290) which resulted in retinal degeneration and was renamed BXD24b/TyJ [21]. Several additional strains were excluded due to abnormally high *Gfap* levels observed in our Full HEI Retina (April 2010) dataset, these include: BXD32, BXD49, BXD70, BXD83 and BXD89.

Tissue preparation protocol.
Mice were killed by rapid cervical dislocation. Retinas were removed immediately and placed in 1 ml of 160 U/ml Ribolock for 1 min at room temperature. The retinas were removed from the eye and placed in Hank's Balanced Salt solution with RiboLock in 50µl RiboLock (Thermo Scientific RiboLock RNase #EO0381 40U/µl 2500U) and stored in -80°C. The RNA was isolated using a QiaCube and the in column DNAse procedure. All RNA samples were checked for quality before running microarrays. The samples were analyzed using the Agilent 2100 Bioanalyzer. The RNA integrity values for ranged from 7.0 to 10. Our goal was to obtain data for independent biological sample pools from both sexes for most lines of mice. The four batches of arrays included in this final data set collectively represent a reasonably well-balanced sample of males and females, in general without within-strain-by-sex replication.

Affymetrix Mouse Gene 2.0 ST Array: These expression arrays have been designed with a median of 22 unique probes per transcript. Each unique probe is 25 bases in length, which means that the array measures a median of 550 bases per transcript. The arrays provide comprehensive transcriptome coverage with over 30,000 coding and non-coding transcripts. In addition there is coverage for over 600 microRNAs. For some arrays the RNA was pooled from two retinas and for other arrays were run on a single retina. Dr. XiangDi Wang (UTHSC) and Rebecca King (Emory) were involved in the retinal extractions and isolation of RNA. The Affymetrix arrays were run by two different research cores: the Molecular Resource Center at UTHSC (Dr. William Taylor Director) and the Integrated Genomics Core at Emory University by Robert B. Isett (Dr. Michael E.

Zwick, Director). In a separate set of experiments we tested a set of arrays from C57BL/6J retinas run at each facility to determine if there were batch effects or other confounding differences in the results. We could not detect any significant difference in the arrays run at UTHSC or at Emory University. Thus, we have included both sets of data into the analysis.

RESULTS

The DoD CDMRP Retina Database presents the retinal transcriptome profiles of 52 BXD RI strains in a highly interactive website, GeneNetwork. There are two separate presentations of the microarray data. The first is at the gene level (DoD CDMRP Retina Affy MoGene 2.0 ST (May15) RMA Gene Level Database) and the same data presented at the exon level (DoD CDMRP Retina Affy MoGene 2.0 ST (May15) RMA Exon Level Database). For the analysis of these dataset there is a suite of bioinformatics tools integrated into the GeneNetwork website. These tools allow for: the identification of genes that vary across the BXD RI strains, the construction of genetic networks controlling the development of the mouse retina, and the identification of genomic loci underlying complex traits in the retina. In the present paper we present these two new datasets and illustrate their use with two examples. The first was to identify genetic signatures of the retinal pigment epithelium (RPE). The second will identify a genetic network associated with roundabout homolog 2 (*Robo2*) gene and the modulating axonal growth.

Cellular Signature of RPE in the DoD CDMRP Retina Database

The DoD CDMRP Retina Database has a unique signature for RPE cells. When looking at the expression of the RPE marker *Rpe65* there was an almost biphasic distribution of expression (Figure 1). Many of the strains expressed relatively low levels of *Rpe65* (approximately 7 units on our scale) while other strains had high levels of expression ranging from 2 to 8 fold higher (8 to 11 units). When we examined the dataset for genes with similar expression across the BXD strains, a list of genes uniquely expressed in RPE was observed (Table 1). This cellular signature represents genes that are uniquely expressed within the RPE, including: *Rgr* (retinal G protein coupled receptor), *Lrat* (Lecithin-retinol acyltransferase), *Rdh5* (retinol deydrogenase 5), *Trf* (transferrin) and *Rrh* (retinal pigment epithelium derived rhodopsin homolog). This signature can also be thought of as the result of genetic networks that drive gene expression within a given cell type. With the new Affymetrix chip we not only have protein-coding genes that correlate with *Rpe65*, but we also have microRNAs and non-coding RNAs. If we examine the top 500 correlates of *Rpe65* (all of which have a correlation higher than 0.8 with *Rpe65*), there are five microRNAs present: *Mir98*, *Mir666*, *Mir449a*, *Mir301b* and *Mir28b*. Using the bioinformatics tools on

TargetScan (Targetscan.org) [22-24] we were able to predict targets for each of the microRNAs from the top 500 correlates of *Rpe65*. One microRNA, *Mir666* did not appear on the Targetscan website. The remaining 4 microRNAs did appear on the website. When scanned for targets *Mir98* had 29 targets in the RPE signature, *Mir449a* had14 targets, *Mir301b* had 13 targets and *Mir28b* had 1 target. This type of analysis may be one approach to constructing and understanding microarray networks within a specific cell type like the RPE of the mouse.

Example of a functional network in the DoD CDMRP Retina Database

To illustrate the features of the new DoD CDMRP Retina Database, we have chosen one specific gene, *Robo2* (roundabout homolog 2), and will use this gene to demonstrate the analytical powers of the database and the bioinformatics tools associated with GeneNetwork. *Robo2* is highly expressed in the retina with a mean value of 10.7 across the BXD strain set. The expression within individual strains varies from a low of 10.2 to a high of 11.1. This is a $\log_2$ scale and represents approximately a two-fold difference in expression (Figure 2). When we examine the database for genes with a similar pattern of expression across the BXD strain set, there is a group of genes that are highly correlated with the expression pattern of *Robo2* (Table 3). One example is the third correlate on the list, *Ncam2* (Figure 3) with a value of 0.926. Even the 100th correlate on the list (*Git1*) has a relatively high correlation (r = 0.873) with *Robo2* (See Supplemental Table 1).

To define the regions of the genome modulating the expression of *Robo2,* we plotted a genome wide scan for *Robo2* (Figure 4). This plot defines regions of the genome that correlate with the level of *Robo2* expression, a quantitative trait locus (QTL). In this interval map there is one significant QTL on chromosome 16 (notice the peak reaches the red line on the scan, p = 0.5) and there are two suggestive peaks on Chromosome 1 and Chromosome 17 (above the gray line). The expression of *Robo2* is modulated by genomic elements on Chromosome 16. There are two types of elements that could be affecting the expression of *Robo2*; a cis-QTL or a gene with a nonsynonymous SNP. If we examine the significant QTL on Chromosome 16 (21-27 Mb), we find there are no significant cis-QTLs at the gene level. With the DoD CDMRP Retina Database it is now possible to look at the individual probes in exons and introns. When we interrogate the DoD CDMRP Retina Exon Level Database, we find one probe (*Affy_17329472*) that lies within the *Leprel1* gene. When we checked the location of the probe with the Verify function on GeneNetwork, the probe lies in an intron and may be a non-coding RNA. However when we examined the RNA-

seq data from GeneNetwork it appears that this was detected in an RNA-seq analysis of the hippocampus and thus this may be part of *Leprel1* gene itself. Nonetheless, this probe marks a candidate for modulating the expression of *Robo2*. The second approach is to examine this region for nonsynonymous SNPs. Using the SNP browser in GeneNetwork, we looked at Chromosome 16 (21-27 Mb) and found four known genes with nonsynonymous SNPs: *Kng2*, *Kng1*, *BC106179* and *Masp1*. This analysis provides us with five candidates for modulating the expression of *Robo2*.

To determine whether this highly correlated set of genes in the *Robo2* network have functional relationship(s), we examined the top 500 correlates of *Robo2* to determine if there were specific functional transcript enrichments using Gene Set (WEB-based GEne SeT AbaLysis Toolkit, http://bioinfo.vanderbilt.edu/webgestalt/webgestalt.php). The list of the top 500 correlates of *Robo2* was enriched for a number of biological processes (nervous system development, synaptic transmission and neuron differentiations); molecular functions (enzyme binding, PDZ domain binding, inorganic cation transmembrane transporter, and metal ion transmembrane transporter activity); and cellular components (cell projection part, neuron projection, intracellular part, and axon genes). This type of analysis plays a critical role in many genetic networks, defining the functional role of the network. In this specific case the analysis demonstrates that the *Robo2* network is involved in axonal growth and neuronal development.

DISCUSSION

This paper announces the release of two new BXD retina databases on GeneNetwork. The first is at the gene level (DoD CDMRP Retina Affy MoGene 2.0 ST (May15) RMA Gene Level Database). The second dataset is exon level analysis of the same data presented in the first dataset (DoD CDMRP Retina Affy MoGene 2.0 ST (May15) RMA Exon Level Database). In this paper we attempt to emphasize some of the special aspects of these two datasets including an exon level of analysis, the inclusion of microRNAs and many non-coding RNAs. To illustrate many of these new features we presented two different approaches for analysis using the datasets.

The first was an examination of a cell signature within the dataset. Within the DoD CDMRP Retina Database, there is a pronounced RPE signature. Some strains demonstrate very low levels of expression of *RPE65* while other strains have over 16-fold higher levels of expression. This difference could not be due to differences in expression within the RPE, for we know that all RPE cells express this gene at approximately the same level. We believe that this is due to differences in the time of day the retinas were isolated. The retinal samples at two different locations. At the University of Tennessee samples were usually isolated starting at 10:00 AM and lights on in the animal colony occurred at 6:00 AM. Thus, the retinas were isolated at least four hours after lights on. At Emory University, the retinas were isolated starting at 9:00 AM and lights on occurred at

7:00 AM or starting at 2 hours after lights on in the animal colony. These differences in the time of day the retinas were isolated may be related to the number of RPE adhering to the retinal samples [25].

There are a number of bioinformatics tools available to the vision research community. These include NEI Bank project (http://neibank.nei.nih.gov/index.shtml), which provides transcriptome profiling of the tissues of the eye including mouse and human [26]. The Cepko group has provided the mouse retina serial analysis of gene expression (SAGE) library (http://itstgp01.med.harvard.edu/retina) that includes gene expression of the embryonic and postnatal retina [27, 28]. Steve Dager and his group have lists of mapped loci and cloned genes associated with inherited retinal disease on the RetNet website (www.sph.uth.tmc.edu/RetNet/). GENSAT (Gene Expression Nervous System Atlas) now has a section devoted to the Retina Project [29] at www.gensat.org/retina.jsp . The cell specific labeling in the retina for different genes is illustrated using BAC transgenic mice. The pattern of labeling in the retina defines the retinal cells types expressing specific genes. This cellular localization aids in defining localization of genetic networks in the retina. Finally we have posted the data from the study of glaucoma by Howell et al.[30] on the GeneNetwork website under the BXD eye database. These data are very helpful in understanding the role of specific genetic networks in glaucoma (for example, see Templeton et al.[31]).

In conclusion, the DoD CDMRP Retina Databases offered on GeneNetwork is new resource in an expanding variety of bioinformatics tools available to vision research community. Previously we have offered several BXD microarray databases on GeneNetwork included to the vision science community: the transcriptome of the whole eye (Eye M430v2 (Sep08) RMA Database) described in detail by Geisert et al.[18]; a normal retina database (Normal Retina (April 2010) RankInv Database) described in detail by Freeman et al.[19]; and the retina 2 days after optic nerve crush (ONC Retina (April 2012) RankInv Database) described in Templeton et al. [32]. This new website offers a unique look at expression at the exon level. In addition, there are many non-protein coding transcripts represented in the dataset. The bioinformatics tools offered on GeneNetwork and these new databases are a unique resource for the vision research community.

Acknowledgments

This work is supported by DoD CDMRP Grant W81XWH1210255 from the U.S. Army Medical Research & Materiel Command and the Telemedicine and Advanced Technology (to EEG), NIH Grant R01EY017841 (to EEG), Vision Core Grant P030EY006360 (to P Michael Iuvone), and Unrestricted Funds from Research to Prevent Blindness (to Emory University). We would like to thank XiangDi Wang for her technical assistance in the early phases of this work.

REFERENCES

1. Consortium, E.P., et al., *Identification and analysis of functional elements in 1% of the human genome by the ENCODE pilot project.* Nature, 2007. **447**(7146): p. 799-816.
2. Lander, E.S., et al., *Initial sequencing and analysis of the human genome.* Nature, 2001. **409**(6822): p. 860-921.
3. Pennisi, E., *Genomics. ENCODE project writes eulogy for junk DNA.* Science, 2012. **337**(6099): p. 1159, 1161.
4. Rubin, G.M., et al., *Comparative genomics of the eukaryotes.* Science, 2000. **287**(5461): p. 2204-15.
5. Venter, J.C., et al., *The sequence of the human genome.* Science, 2001. **291**(5507): p. 1304-51.
6. Redmond, T.M., et al., *Rpe65 is necessary for production of 11-cis-vitamin A in the retinal visual cycle.* Nat Genet, 1998. **20**(4): p. 344-51.
7. Allikmets, R., et al., *Mutation of the Stargardt disease gene (ABCR) in age-related macular degeneration.* Science, 1997. **277**(5333): p. 1805-7.
8. Nathans, J. and D.S. Hogness, *Isolation and nucleotide sequence of the gene encoding human rhodopsin.* Proc Natl Acad Sci U S A, 1984. **81**(15): p. 4851-5.
9. Swaroop, A., et al., *Leber congenital amaurosis caused by a homozygous mutation (R90W) in the homeodomain of the retinal transcription factor CRX: direct evidence for the involvement of CRX in the development of photoreceptor function.* Hum Mol Genet, 1999. **8**(2): p. 299-305.
10. Bork, J.M., et al., *Usher syndrome 1D and nonsyndromic autosomal recessive deafness DFNB12 are caused by allelic mutations of the novel cadherin-like gene CDH23.* Am J Hum Genet, 2001. **68**(1): p. 26-37.
11. Adato, A., et al., *Mutation profile of all 49 exons of the human myosin VIIA gene, and haplotype analysis, in Usher 1B families from diverse origins.* Am J Hum Genet, 1997. **61**(4): p. 813-21.
12. Stone, E.M., et al., *Identification of a gene that causes primary open angle glaucoma.* Science, 1997. **275**(5300): p. 668-70.
13. Crooks, K.R., et al., *Genome-wide linkage scan for primary open angle glaucoma: influences of ancestry and age at diagnosis.* PLoS One, 2011. **6**(7): p. e21967.
14. Ulmer, M., et al., *Genome-wide analysis of central corneal thickness in primary open-angle glaucoma cases in the NEIGHBOR and GLAUGEN consortia.* Invest Ophthalmol Vis Sci, 2012. **53**(8): p. 4468-74.

15. Aung, T., et al., *A common variant mapping to CACNA1A is associated with susceptibility to exfoliation syndrome.* Nat Genet, 2015. **47**(4): p. 387-92.
16. Scheetz, T.E., et al., *A genome-wide association study for primary open angle glaucoma and macular degeneration reveals novel Loci.* PLoS One, 2013. **8**(3): p. e58657.
17. Grassi, M.A., et al., *Complement factor H polymorphism p.Tyr402His and cuticular Drusen.* Arch Ophthalmol, 2007. **125**(1): p. 93-7.
18. Geisert, E.E., et al., *Gene expression in the mouse eye: an online resource for genetics using 103 strains of mice.* Molecular vision, 2009. **15**: p. 1730-63.
19. Freeman, N.E., et al., *Genetic networks in the mouse retina: growth associated protein 43 and phosphatase tensin homolog network.* Mol Vis, 2011. **17**: p. 1355-72.
20. Peirce, J.L., et al., *A new set of BXD recombinant inbred lines from advanced intercross populations in mice.* BMC Genet, 2004. **5**: p. 7.
21. Chang, B., et al., *In-frame deletion in a novel centrosomal/ciliary protein CEP290/NPHP6 perturbs its interaction with RPGR and results in early-onset retinal degeneration in the rd16 mouse.* Hum Mol Genet, 2006. **15**(11): p. 1847-57.
22. Garcia, D.M., et al., *Weak seed-pairing stability and high target-site abundance decrease the proficiency of lsy-6 and other microRNAs.* Nat Struct Mol Biol, 2011. **18**(10): p. 1139-46.
23. Grimson, A., et al., *MicroRNA targeting specificity in mammals: determinants beyond seed pairing.* Mol Cell, 2007. **27**(1): p. 91-105.
24. Lewis, B.P., C.B. Burge, and D.P. Bartel, *Conserved seed pairing, often flanked by adenosines, indicates that thousands of human genes are microRNA targets.* Cell, 2005. **120**(1): p. 15-20.
25. Ruggiero, L., et al., *alphavbeta5 integrin-dependent diurnal phagocytosis of shed photoreceptor outer segments by RPE cells is independent of the integrin coreceptor transglutaminase-2.* Adv Exp Med Biol, 2012. **723**: p. 731-7.
26. Wistow, G., *The NEIBank project for ocular genomics: data-mining gene expression in human and rodent eye tissues.* Prog Retin Eye Res, 2006. **25**(1): p. 43-77.
27. Blackshaw, S., et al., *Genomic analysis of mouse retinal development.* PLoS Biol, 2004. **2**(9): p. E247.
28. Blackshaw, S., et al., *Comprehensive analysis of photoreceptor gene expression and the identification of candidate retinal disease genes.* Cell, 2001. **107**(5): p. 579-89.
29. Siegert, S., et al., *Genetic address book for retinal cell types.* Nat Neurosci, 2009. **12**(9): p. 1197-204.
30. Howell, G.R., et al., *Molecular clustering identifies complement and endothelin induction as early events in a mouse model of glaucoma.* J Clin Invest, 2011. **121**(4): p. 1429-44.
31. Templeton, J.P., et al., *Innate immune network in the retina activated by optic nerve crush.* Invest Ophthalmol Vis Sci, 2013. **54**(4): p. 2599-606.
32. Templeton, J.P., et al., *A crystallin gene network in the mouse retina.* Exp Eye Res, 2013. **116**: p. 129-40.

Figures

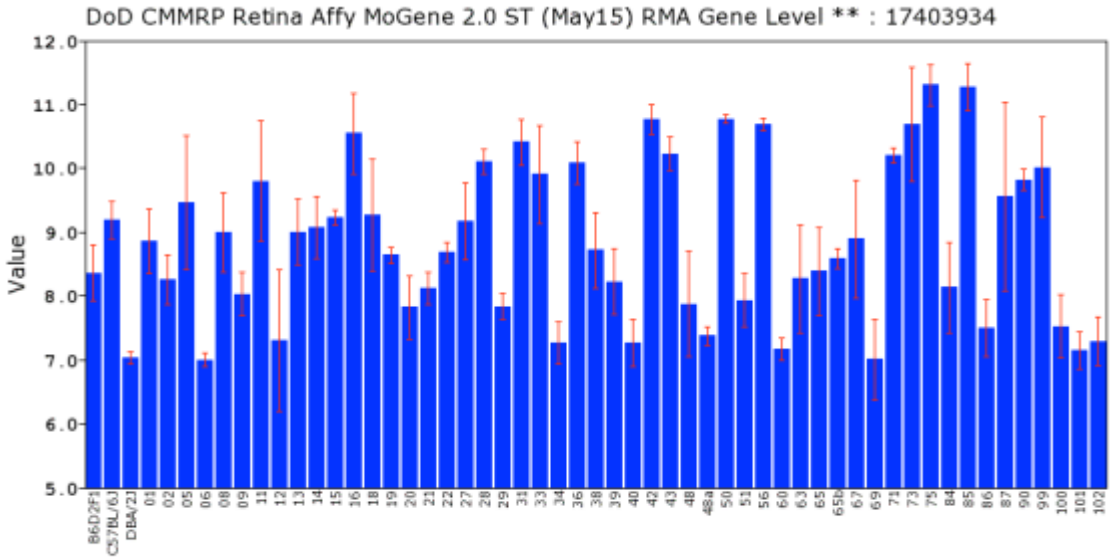

Figure 1 Expression of *Rpe65* across the BXD strains in the DoD CDMRP Normal Retina Dataset. The expression levels of *Rpe65* are shown for many of the BXD strains as mean expression and standard error of the mean. The individual strain identifications are shown along the bottom and the scale is $\log_2$. Notice the relatively low levels of *Rpe65* in some stains (DBA/2J, BXD5 BXD12, BXD34, BXD40, BXD48a, BXD60, BXD69, BXD100, BXD101 and BXD102) and 8-fold high levels of expression other strains (BXD16, BXD31, BXD42, BXD43, BXD50, BXD56, BXD75 and BXD85).

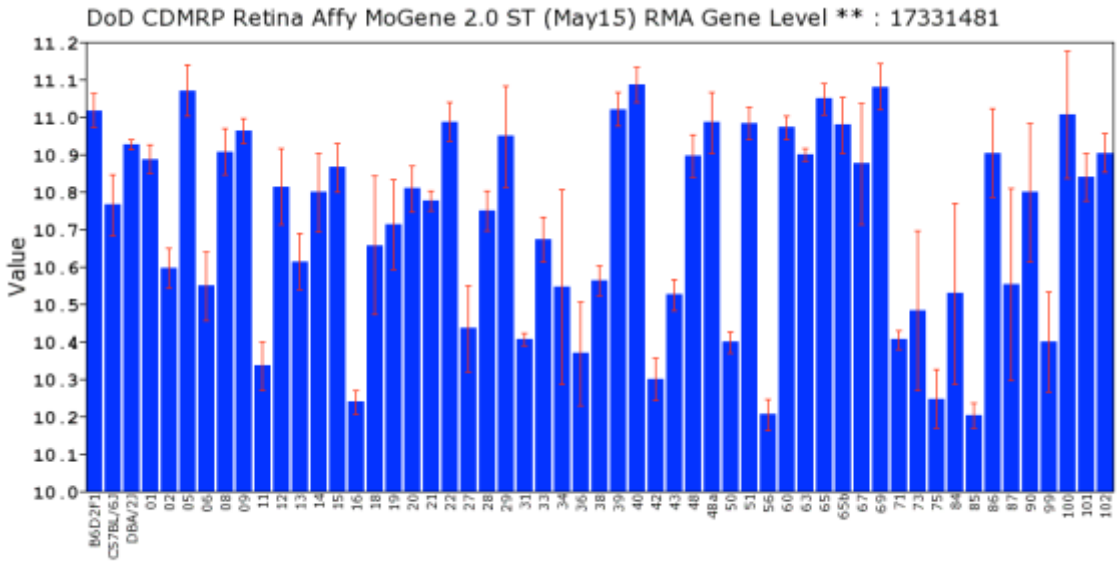

Figure 2 Expression of *Robo2* across the BXD strains in the DoD CDMRP Normal Retina Dataset. The expression levels of *Robo2* are shown for many of the BXD strains as mean expression and standard error of the mean. The individual strain identifications are shown along the bottom of the plot and the scale is $\log_2$. Notice the variability in *Robo2* expression across the BXD strains.

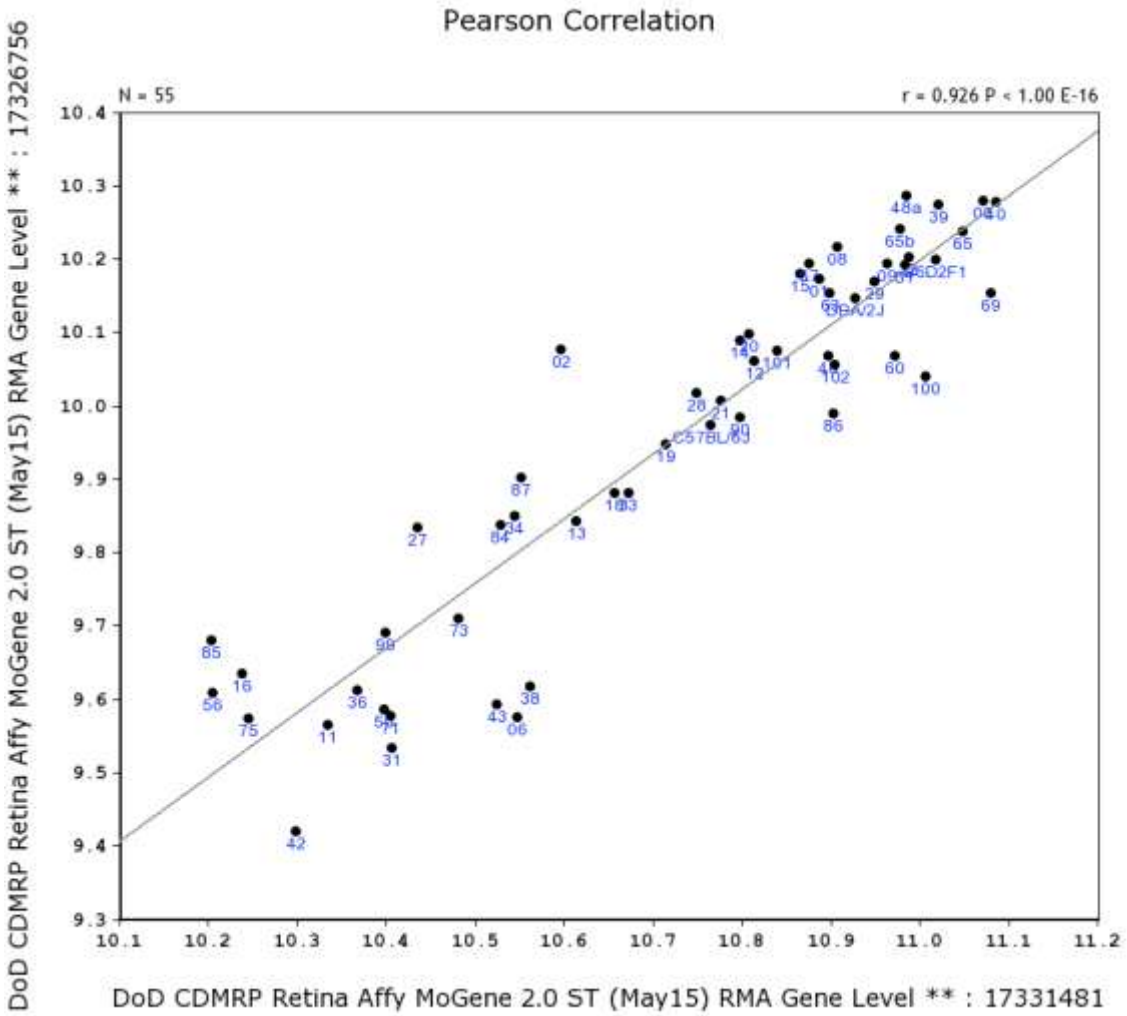

Figure 3 The Pearson correlation between *Robo2* and *Ncam2*. *Ncam2* was the second highest correlate to *Robo2* in the DoD CDMRP. Notice that in strains where *Robo2* is highly expressed, *Ncam2* is also highly expressed and that in strains where *Robo2* is low, *Ncam2* is also low.

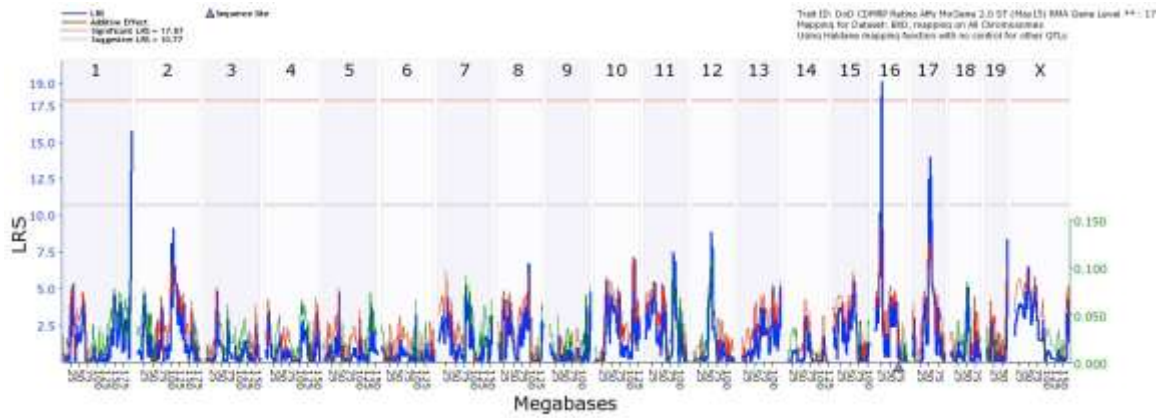

Figure 4. Genome-wide Interval Map of *Robo2*. This genome-wide graph displays the quantitative trait loci (QTL) distribution across the DoD CDMRP Normal Retina Dataset. The X-axis plots the locations of the QTLs controlling the transcript expression. Positions are measured in mega-bases from Chromosome 1 to Chromosome X (1-2600 Mb). The *y*-axis plots Likelihood Ratio Statistic (LRS). The significant levels of individual QTLs are color-coded. The red line represents a genome-wide significance level ($p > 0.05$) and the gray line is suggestive. Notice a significant QTL on Chromosome 16.

Table 1. Correlates of *Rpe65* in the DoD CDMRP Normal Retina Dataset.

Symbol	Description	Location (Chr: Mb)	Mean Expr	Sample r
Rpe65	retinal pigment epithelium 65	Chr3: 159.262145	8.837	1.000
Rgr	retinal G protein coupled receptor	Chr14: 37.850676	10.660	0.985
Pon1	paraoxonase 1	Chr6: 5.118090	7.608	0.976
Ttr	transthyretin	Chr18: 20.823751	10.858	0.946
Ermn	ermin, ERM-like protein	Chr2: 57.897524	7.173	0.938
Lrat	lecithin-retinol acyltransferase	Chr3: 82.696501	8.190	0.935
Rdh5	retinol dehydrogenase 5	Chr10: 128.350646	8.763	0.924
Slc6a20a	solute carrier family 6, member 20A	Chr9: 123.545240	8.364	0.916
Trf	transferrin	Chr9: 103.106331	10.660	0.891
Slc26a7	solute carrier family 26, member 7	Chr4: 14.429577	7.979	0.891
Car12	carbonic anyhydrase 12	Chr9: 66.561493	7.904	0.890
Clstn1	calsyntenin 1	Chr4: 148.960577	12.739	-0.879
Camk2b	calcium	Chr11: 5.869645	8.982	-0.879
Pkm	pyruvate kinase, muscle	Chr9: 59.504175	13.461	-0.876
Thbs1	thrombospondin 1	Chr2: 117.937612	8.372	0.875
Abl1	c-abl oncogene 1, non-receptor tyrosine kinase	Chr2: 31.543896	8.803	-0.873
Itgb8	integrin beta 8	Chr12: 120.396495	9.948	0.873
Rrh	retinal pigment epithelium derived rhodopsin homolog	Chr3: 129.507326	10.405	0.873
Tiam1	T-lymphoma invasion and metastasis-inducing	Chr16: 89.787356	9.161	-0.873
Chchd3	coiled-coil-helix-coiled-coil-helix domain containing 3	Chr6: 32.740976	10.721	0.869
Gm5567	predicted gene 5567	Chr6: 40.060252	9.840	-0.869
Hdac5	histone deacetylase 5	Chr11: 102.086139	10.804	-0.868
Cntn2	contactin 2	Chr1: 134.406002	8.840	-0.868
Olfr875	olfactory receptor 875	Chr9: 37.580222	7.601	0.866
Gm19522	predicted gene, 19522	Chr16: 42.884483	7.568	0.866
Sez6l2	seizure related 6 homolog like 2	Chr7: 134.094049	10.136	-0.863
Nrxn2	neurexin II	Chr19: 6.418731	10.141	-0.862
Olfr726	olfactory receptor 726	Chr14: 50.703389	7.145	0.862
Sv2a	synaptic vesicle glycoprotein 2 a	Chr3: 95.985074	12.282	-0.861
Tmem161b	transmembrane protein 161B	Chr13: 84.361901	10.910	0.861
Pdcd5	programmed cell death 5	Chr1: 191.101187	11.261	0.860
Fap	fibroblast activation protein	Chr2: 62.339000	7.186	0.860
Cacna1g	calcium channel, voltage-dependent	Chr11: 94.269705	9.954	-0.860
Rapgef1	Rap guanine nucleotide exchange factor (GEF) 1	Chr2: 29.475240	10.495	-0.859
Nsmce2	non-SMC element 2 homolog	Chr15: 59.205753	10.909	0.859
Plxna1	plexin A1	Chr6: 89.266307	10.088	-0.858
Ube2b	ubiquitin-conjugating enzyme E2B	Chr11: 51.798648	11.282	0.858
Aacs	acetoacetyl-CoA synthetase	Chr5: 125.956184	9.520	-0.857
Acsf3	acyl-CoA synthetase family member 3	Chr8: 125.299405	9.514	-0.856
Slc17a7	solute carrier family 17, member 7	Chr7: 52.419291	13.143	-0.856
Srebf2	sterol regulatory element binding factor 2	Chr15: 81.977696	11.306	-0.855
Epb4.9	erythrocyte protein band 4.9	Chr14: 71.001070	9.983	-0.855
Vapa	vesicle-associated membrane protein, associated protein A	Chr17: 65.929392	12.315	0.855
Slc12a5	solute carrier family 12, member 5	Chr2: 164.786302	12.122	-0.854
Card9	caspase recruitment domain family, member 9	Chr2: 26.207696	7.648	-0.854
Cfh	complement component factor h	Chr1: 141.982432	8.586	0.853
Dagla	diacylglycerol lipase, alpha	Chr19: 10.319755	9.568	-0.853
Pde4dip	phosphodiesterase 4D interacting protein (myomegalin)	Chr3: 97.493751	9.553	-0.853
Ank1	ankyrin 1, erythroid	Chr8: 24.085316	9.543	-0.853
Zcchc14	zinc finger, CCHC domain containing 14	Chr8: 124.122603	10.388	-0.853
Ssr3	signal sequence receptor, gamma	Chr3: 65.186870	6.086	0.853
Mterfd1	MTERF domain containing 1	Chr13: 67.007904	9.547	0.853
Apba1	amyloid beta (A4) precursor protein binding, A, member 1	Chr19: 23.833366	10.554	-0.852
Acot13	acyl-CoA thioesterase 13	Chr13: 24.909817	10.632	0.851
Rbl1	retinoblastoma-like 1 (p107)	Chr2: 156.971629	9.071	0.851
Cpxm2	carboxypeptidase X 2 (M14 family)	Chr7: 139.234493	8.069	0.851
Ret	ret proto-oncogene	Chr6: 118.101766	10.226	-0.850
Mospd1	motile sperm domain containing 1	ChrX: 50.698185	10.714	0.850
Lrp3	low density lipoprotein receptor-related protein 3	Chr7: 35.984852	9.102	-0.850

Table 2. MicroRNAs in the *Rpe65* signature.

Rpe65	Mir98	Mir449a	mir301b	mir28b
Camk2b	--	--	--	Camk2b
Atp2b2	--	--	Atp2b2	--
Cfl2	--	--	Cfl2	--
Dlc1	--	--	Dlc1	--
Eif2c1	Eif2c1	--	Eif2c1	--
Nptx1	Nptx1	Nptx1	Nptx1	--
Pitpnm2	--	--	Pitpnm2	--
Ppp6r1	--	--	Ppp6r1	--
Psap	--	--	Psap	--
Slc17a7	--	--	Slc17a7	--
Snx2	--	--	Snx2	--
Sub1	--	--	Sub1	--
Tet3	--	--	Tet3	--
Zbtb4	--	--	Zbtb4	--
Zcchc14	--	--	Zcchc14	--
2610507B11Rik	2610507B11Rik	2610507B11Rik	--	--
Abr	Abr	Abr	--	--
Ahsa2	Ahsa2	Ahsa2	--	--
Cacna2d2	Cacna2d2	Cacna2d2	--	--
Cntn2	Cntn2	Cntn2	--	--
Dcaf7	Dcaf7	Dcaf7	--	--
E2f5	E2f5	E2f5	--	--
Fbxo10	Fbxo10	Fbxo10	--	--
Mgat5b	Mgat5b	Mgat5b	--	--
Ndst1	Ndst1	Ndst1	--	--
Nrxn2	Nrxn2	Nrxn2	--	--
Pvrl1	Pvrl1	Pvrl1	--	--
Ret	Ret	Ret	--	--
Slc6a1	Slc6a1	Slc6a1	--	--
Tfdp2	Tfdp2	Tfdp2	--	--
Trim67	Trim67	Trim67	--	--
Usp31	Usp31	Usp31	--	--
Agap1	Agap1	--	--	--
Apba1	Apba1	--	--	--
Bsn	Bsn	--	--	--
Fbxl14	Fbxl14	--	--	--
Insr	Insr	--	--	--
Kcnc1	Kcnc1	--	--	--
Nsmce2	Nsmce2	--	--	--
Slc7a14	Slc7a14	--	--	--
Srebf2	Srebf2	--	--	--
Syt7	Syt7	--	--	--
Thbs1	Thbs1	--	--	--

Table 3. Top 20 correlates of *Robo2*.

Symbol	Description	Location (Chr: Mb)	Mean Expr	Sample r
Robo2	roundabout homolog 2 (Drosophila)	Chr16: 73.892551	10.72	1.00
Cask	calcium	ChrX: 13.094206	10.91	0.94
Ncam2	neural cell adhesion molecule 2	Chr16: 81.200942	9.95	0.93
Gria3	glutamate receptor, ionotropic, AMPA3	ChrX: 38.754305	10.25	0.92
Lphn3	latrophilin 3	Chr5: 81.450227	10.25	0.92
Cnksr2	connector enhancer of kinase suppressor of Ras 2	ChrX: 154.259368	10.37	0.92
Clstn2	calsyntenin 2	Chr9: 97.344814	10.00	0.92
Gnaq	guanine nucleotide binding protein	Chr19: 16.207321	10.63	0.92
Dnajc6	DnaJ (Hsp40) homolog, subfamily C, member 6	Chr4: 101.169253	11.97	0.92
Slc8a1	solute carrier family 8 (sodium	Chr17: 81.772445	9.45	0.91
Dpysl2	dihydropyrimidinase-like 2	Chr14: 67.421701	13.25	0.91
Plch1	phospholipase C, eta 1	Chr3: 63.500156	10.96	0.91
Gria1	glutamate receptor, ionotropic, AMPA1 (alpha 1)	Chr11: 56.824889	9.77	0.91
Fam165b	family with sequence similarity 165, member B	Chr16: 92.301531	10.04	-0.91
Ncam1	neural cell adhesion molecule 1	Chr9: 49.310243	12.95	0.90
B4galt6	UDP-Gal:betaGlcNAc beta 1,4-galactosyltransferase	Chr18: 20.843100	10.76	0.90
Odz1	odd Oz	ChrX: 40.677132	8.81	0.90
Sort1	sortilin 1	Chr3: 108.087009	11.52	0.90
Ubqln2	ubiquilin 2	ChrX: 149.932775	11.29	0.90
Mtmr9	myotubularin related protein 9	Chr14: 64.142447	11.71	0.90
Gabbr2	gamma-aminobutyric acid (GABA) B receptor, 2	Chr4: 46.675190	11.04	0.90

Upregulation of SOX11 in Retinal Ganglion Cells Following Injury

Felix L. Struebing[1], Steven G. Hart[2,3], Joseph M. Caron[2,4], XiangDi Wang[2] and Eldon E. Geisert[1]

[1]Department of Ophthalmology, Emory University 1365B Clifton Road NE Atlanta GA, 30322, [2]Department of Ophthalmology, University of Tennessee Health Science Center, 930 Madison Ave. Memphis, TN 38163

Corresponding Author:
Eldon E. Geisert
Professor of Ophthalmology
Emory University
1365B Clifton Road NE
Atlanta GA 30322
email: egeiser@emory.edu
Phone: 404-778-4239

[3]Current address:

[4]Current address:

Abstract

Purpose: The present study was designed to identify early changes associated with injury of retinal ganglion cells.

Methods: The normal retina database and optic nerve crush (ONC) database on GeneNetwork (www.genenetwork.org) were used to identify markers of retinal injury. One gene, *Sox11*, was examined further using two neuronal injury paradigms, ONC and blast injury to the eye of C57BL/6 mice. The distribution of SOX11 was determined using indirect immunohistochemical methods and the levels of SOX11 protein expression were defined by semi-quantitative immunoblot methods. *In situ* hybridization was performed using the Affymetrix 2-plex Quantigene View RNA In Situ Hybridization Tissue Assay System.

Results: SOX11 was dramatically upregulated in the retina following ONC and blast injury. The level of *Sox11* message increased by approximately 8-fold 2 days after ONC. In the normal retina, there was only light immunostaining for SOX11 in retinal ganglion cells and cells in the inner nuclear layer. After ONC or blast injury, the staining intensity increased dramatically in both layers. In situ hybridization demonstrated a similar distribution of message for *Sox11* in the normal retina as well as a profound increase in *Sox11* message within the ganglion cells following ONC.

Conclusion: Taken together, these data indicate that *Sox11* may be involved in the initial response of the retina to injury, playing a role in the early attempts of the ganglion cells to survive.

Introduction:

Advances in our ability to monitor molecular changes in neurons have led to an increased understanding of the events that transpire following neuronal injury [1-5]. After axonal damage, the initial response of a central nervous system (CNS) neuron may be similar to that of a neuron in the peripheral nervous system (PNS) [6]. Ultimately, neurons in the PNS will regenerate their axons and survive, while those in the CNS do not regenerate their axons and the cell bodies die. The initial response of the CNS neurons to regenerate and eventual failure of this regenerative response was described by Ramón y Cajal and termed “abortive regeneration” [7]. When examining the initial response of neurons to injury, there appear to be some common responses in the CNS and PNS. One transcription factor activated in both the CNS and PNS after injury is *Sox11* [8]. There is strong evidence that this gene is part of the transcriptional network activated by injury and involved in axonal regeneration in the PNS [9, 10].

Sox11 is a member of the SRY-related box group C (*SoxC*) gene family of transcription factors [11, 12]. SOX11 along with SOX4 play a critical role in the normal development of neurons and specifically retinal ganglion cells [13-15]. SOX11 is expressed in retinal progenitor cells as part of the process leading progenitor cells to become neuroblasts [16, 17]. In knock-downs of either *Sox11* or *Sox4*, there is a moderate reduction in retinal ganglion cell number; however when both *Sox11* and *Sox4* are knocked-down, there is a complete loss of ganglion cell development [13]. During eye development, *Sox11* is also required to maintain proper levels of *hedgehog* signaling, and mutations have been associated with coloboma due to improper optic fissure closure [18, 19]. Furthermore, SOX11 is critical for axonal growth, driving the expression of axon growth-related proteins such as class III beta tubulin and MAP2 [20]. SOX11 also plays a similar role in adult neurogenesis. High levels of SOX11 are found in the cells within the subventricular zone, the rostral migratory stream and within the

neuroprogenitor zone of the dentate gyrus [15, 16, 21]. These studies underline the importance of SOX11 in terminal differentiation of progenitor cells to neurons and axon extension.

In addition to functioning in neuronal differentiation, SOX11 has a prominent role in the response of neurons to injury. After peripheral nerve injury, SOX11 is immediately upregulated in the neuronal cell bodies as the axon is regenerating [9, 22]. Decreasing levels of SOX11 in the neuronal cell body results in slower axonal regeneration of peripheral nerves [9]. Similar results are observed in tissue culture. When *Sox11* is knocked down in cultured peripheral neurons, there is also a reduction in neurite growth and an increase in apoptosis [23]. Conversely, overexpressing *Sox11* in cultured dorsal root ganglion cells produces an increase in neurite growth, and *in vivo* overexpression of *Sox11* accelerates the growth of regenerating axons [10]. One intriguing anatomical experimental model is the dorsal root ganglion, where the central projection of the dorsal root ganglion enters the spinal cord (CNS) and the peripheral projection extends out into a peripheral nerve that is myelinated by Schwann cells. When the central rootlet is severed, there is a modest (51%) increase in *Sox11* expression in the ganglion even when the central portion will not regenerate back into the spinal cord. However, when the peripheral root is damaged, a relatively massive (1004%) increase in *Sox11* is seen as the axons regenerate down the peripheral nerve.

In the present study, we examine the role of SOX11 in the retina following injuries to the axons of the optic nerve. We propose that the upregulation of SOX11 after injury is an attempt of neurons to regenerate, but ultimately results in abortive regeneration and cell death.

Materials and Methods

Optic Nerve Crush. The Optic Nerve Crush procedure was performed as previously described in Templeton et al [24]. Briefly, C57BL/6 (n = 5) mice were deeply anesthetized with 13 mg/kg Rompum and 87 mg/kg Ketalar for the surgery. An incision was made into the lateral aspect of the conjunctiva, and the eye was rotated nasally to expose the optic nerve. The optic nerve was then grasped for 10 seconds with Dumont cross-clamp #7 forceps (Roboz, cat. #RS=5027, Gaithersburg, MD), using only the spring action of the instrument to crush the nerve. The instrument was then removed and the eye was allowed to rotate back into place. The animals were allowed to recuperate from surgery on a water-heated warming pad. The Institutional Animal Care and Use Committee approved all procedures for the surgery and handling of mice (at the University of Tennessee Health Science Center and Emory University).

Blast Injury to the Eye. Blast injuries to the eye were produced as previously reported in Hines-Beard et al [25]. Briefly, the mice were deeply anesthetized and secured in a PVC pipe. A 50psi overpressure wave was delivered selectively to the right eye of C57BL/6 mice (n = 5). The output pressure of the blast apparatus was measured immediately before and after the procedure, ensuring an accurate and precise injury. The animals were sacrificed 5 days after the blast injury. The Institutional Animal Care and Use Committee approved all procedures for the surgery and handling of mice (at the University of Tennessee Health Science Center and Emory University).

Immunoblot Analysis. Protein samples from 12 retinas were examined to determine the relative levels of SOX11. Animals were anesthetized with a mixture of xylazine (13 mg/kg, Rompum) and ketamine (87 mg/kg, Ketalar) and following a cervical dislocation the retinas were removed. The dissected retinas were placed in 1X reducing sample buffer (2% SDS and 10% glycerol in 0.05 M Tris-HCl buffer, pH 6.8). Equal amounts of protein were loaded onto each lane of

an SDS PAGE gel. The balance of the proteins was determined by coomassie blue staining and subsequent quantification of total protein in each lane. To analyze the concentrations of SOX11 in the retina, the proteins were transferred to PVD membranes. The blots were blocked with 2% non-fat dry milk in phosphate buffer (pH 7.4) and probed overnight with the rabbit anti- SOX11 primary antibody (Santa Cruz Biotechnology, Inc. California). We then rinsed the blots and probed them with the HRP-labeled donkey anti-rabbit secondary antibody (Jackson ImmunoResearch Laboratories, Inc., West Grove, Pennsylvania). The blots were rinsed with 0.5 M Tris buffer (pH 7.4) and reacted with 0.05% DAB and hydrogen peroxide. The blots were washed and visualized using an ECL detection kit (Thermo Fisher Scientific Inc. Rockford, Illinois) and Kodak 4000 MM image station. To define the amount of protein loaded onto each lane the blot was stripped and restained for actin using a mouse anti-B-Actin antibody (A5441, Sigma Aldrich, St Louis MO) followed by an HRP-labeled Donkey anti-mouse secondary antibody (Jackson ImmunoResearch Laboratories, Inc., West Grove, Pennsylvania). The blots were then rescanned.

Immunohistochemistry. For the immunohistochemical analysis of the distribution of SOX11, ten C57BL/6 mice (2 control mice and 2 mice of each group at both 2 and 5 days postoperatively) were used. The mice were deeply anesthetized with 2,2,2-tribromoethanol and then perfused transcardially with saline followed by 4% paraformaldehyde using a peristaltic pump (Cole Parmer Instruments, Chicago, IL). After an hour of post-fixation in paraformaldehyde at room temperature, retinas were rinsed in 0.1M phosphate-buffered saline (PBS), embedded in 4% low-melt agarose, and cut on a vibratome into 50 µm thick slices. Sections were then blocked in 4% bovine serum albumin (Sigma-Aldrich, St. Louis, MO) in PBS with 0.1% Triton X-100 (Sigma) on a rotating platform for 1 hour, washed 3 times and incubated with primary antibody at 4°C overnight. The next day, sections were rinsed again and then incubated in Alexa Fluor-conjugated secondary antibody (Life Technologies). After that, sections were rinsed in PBS, mounted with Fluoromount (Southern Biotech, Birmingham, AL)

and coverslipped. The following primary antibodies and dilutions were used: anti-SOX11 (US Biological S5364-40C, 1:500), anti-TUJ1 (Tuj1, a gift from Anthony Franfurter [26]), and anti-PKC alpha (abcam ab32376, 1:250). The following anti-SOX11 antibodies were tried for Immunohistochemistry but did not work: Santa Cruz sc-20096, abcam ab170916, biorbyt 101332, and LifeSpan Biosciences LS-C10306.

Confocal Microscopy. The sections were scanned and 10 µm thick z-stacks were acquired on a Eclipse Ti confocal microscope (Nikon Inc., Melville, NY) equipped with Nikon C1 software. Scans were taken using a 40x Plan Fluor 40x/1.30/0.20 Oil objective. Laser power and gain were kept constant for all pictures. Images were loaded into Fiji [27] and average intensity projections were created. The final composition of the images was made using Photoshop CS 6 (Adobe Systems Inc., San Jose, CA).

***In Situ* Hybridization.** *In situ* hybridization was performed using the 2-plex Quantigene View RNA ISH Tissue Assay kit (Affymetrix, Inc., Santa Clara, California). Assays were performed as per the manufacturer's instructions with stock solutions. Eyes were isolated from C57BL/6 mice (n = 6), both control and two days after optic nerve crush, and drop-fixed in 4% Paraformaldehyde for 24 hours. Mid-way through the 24-hour fixation, a 26-gauge needle was used to create a hole to the vitreous humor, assisting with the fixation. Immediately after the 24-hour period, the eyes were serially dehydrated in ethanol and embedded in paraffin. Blocks were sectioned on an American Optical series 1000 microtome (American Optical Co. Buffalo, New York) to a thickness of 5 µm and mounted on Surgipath X-tra micro slides (Leica Biosystems Richmond Inc., Richmond, Illinois). Before beginning the hybridization protocol, the slides were baked at 60^{o} C for 30 minutes to increase tissue adhesion. As per the manufacturer's protocol, the paraffin was removed from the slides with xylene before being boiled in a pretreatment solution (Affymetrix) for 10 minutes and incubated with Protein

Kinase K [Affymetrix Santa Clara, CA] at 40^{o} C for 10 minutes. Custom probes for *Sox11* and *Chrna6* [Affymetrix Santa Clara, CA] were then hybridized to the tissue. Signal amplification was accomplished by hybridizing Type 1 and Type 2 specific pre-amp oligonucleotides, amp oligonucleotides and label oligonucleotides sequentially, achieving a 400-fold signal amplification from each mRNA molecule. Sections were viewed with an Olympus BX51 microscope (Olympus America Inc., Melville, New York).

Results

We first compared *Sox11* mRNA levels in normal mice to *Sox11* levels following ONC using the bioinformatic tools on GeneNetwork (genenetwork.org) and two preexisting databases generated by us: Normal HEI Retina (April 2010) and ONC HEI Retina (April. 2012) [4, 28]. *Sox11* was one of the genes with the largest change in expression two days after optic nerve crush. In the normal retinal dataset, the mean expression for *Sox11* (detected by Illumina probe ILMN_1235647) across the BXD RI strains was 8.4 on a 2 Z + 8 Log_2 scale (this is just above the mean detection level of mRNA on the array, which is set to 8). In the C57BL/6 parental strain, the expression level in the normal retina was 8.59 and for the DBA/2J strain the mean expression level was 8.54. Two days after ONC, there was a dramatic increase in the level of *Sox11* expression (Figure 1), with the mean expression across the BXD strains being 11.03, which corresponded to an approximately 8-fold increase. The same increase was observed in individual strains. The C57BL/6 strain had an expression level of 11.33 after ONC and the expression in the DBA/2J strain increased to 11.44. These data indicate that *Sox11* is dramatically upregulated after a specific injury to the ganglion cell axons within the optic nerve.

In situ hybridization was used to identify the cells expressing *Sox11* after injury to the retina. For the *in situ* hybridization, we examined retinas two days after optic nerve crush (Fig. 2B) and compared it to uninjured control retinas (Fig. 2A). Using the Affymetrix 2-plex Quantigene View RNA ISH Tissue Assay kit, we labeled cells expressing the retinal ganglion cell marker *Chrna6* blue and *Sox11* red (Fig. 2) [3]. In the control retina, many of the cells in the ganglion cell layer were heavily labeled for *Chrna6*, and a few of the cells expressed low levels of *Sox11*. Two days after optic nerve crush there was a dramatic decrease in the labeling for *Chrna6* and a substantial increase in the amount of labeling for *Sox11*. This was similar to the changes in message levels observed in our microarray databases on GeneNetwork.org. In the normal retina database, *Chrna6* (probe ILMN_2732438) was expressed at relatively high levels (mean

value of 11.04) and two days following optic nerve crush, the expression decreased two-fold (mean value of 9.96). These data from the *in situ* hybridization mirror our microarray expression analysis results.

Indirect immunohistochemistry was used to define the distribution of SOX11 protein in the retina. To identify the cell types expressing SOX11 after retinal injury, we stained the retina for SOX11 and for class III beta tubulin, a known ganglion cell marker [26]. In these double-labeled sections, staining for SOX11 was colocalized with class III beta tubulin in retinal ganglion cells (Fig. 3), indicating that they were also positive for SOX11. Both markers labeled the same population of cells in the ganglion cell layer and the labeling extended out into dendritic processes. The staining pattern also indicated that SOX11 was present in the cytoplasm and the nucleus. Even though nuclear labeling was light in comparison, there were many cases where a negative spot (presumably the nucleolus) could be observed. These data demonstrate that SOX11 is present in injured retinal ganglion cells.

Using immunohistochemistry, we also examined the change in expression of SOX11 following optic nerve crush (Fig 4B and 4C) and a blast injury to the eye (Fig. 4E and 4F). In both cases, there was a noticeable increase in ganglion cell staining relative to that observed in the uninjured control section (Fig. 4A). The staining was primarily cytosolic and extended out into the dendritic processes of the cells. In the normal retina, we could identify light labeling of cells within the inner nuclear layer. The intensity of labeling within the retinal ganglion cells increased dramatically in the injured retinas (Fig. 4B, 4C, 4E and 4F), and there was also an increase in staining of cells within the inner nuclear layer, which colocalized partly to bipolar cells (Fig. 5).

The upregulation of SOX11 following ONC was confirmed with Immunoblotting. The intensity of the SOX11 band from retinas after nerve crush (Fig. 6, lanes A and C) is higher than in the control retina samples (Fig. 6 lanes B and D). Thus,

there is a dramatic increase in the expression of both *Sox11* mRNA and SOX11 protein following retinal injury.

Discussion

In the present study, we demonstrate that SOX11 is upregulated following retinal injury. For retinal ganglion cells, there are many known markers, such as: *Chrna6*, *Pou4f1*, *Tubb3*, *Thy1*, and *Sncg* [3, 13, 29-33]. Using these marker genes, we performed a meta-analysis of their expression in injured and uninjured retinas (data not shown). Our injury paradigms included controlled optic nerve crush and selective blast injury to the eye, procedures that are known to induce retinal ganglion cell apoptosis [24, 25]. As expected, the expression of these retinal ganglion cell markers decreases as the ganglion cells die. Our data indicate an overall reduction in expression of these markers, both 2 and 5 days after retinal insult [34]. Specifically, a 3-fold reduction in *Sncg* expression is observed, *Chrna6* and *Pou4f1* are down regulated 2-fold, and, while not as robust, *Thy1* and *Tubb3* also show a decrease in expression. Collectively, these data demonstrate that known retinal ganglion cell markers decrease as the optic nerve degenerates.

Unlike these markers for retinal ganglion cells, *Sox11* levels increase substantially following injury to the retina and optic nerve. Two days after ONC, there was an almost 8-fold upregulation of *Sox11*. We wondered if this increase in expression was specific to the severity of retinal injury, and queried a publicly available microarray dataset of glaucomatous mice presented by Howell and colleagues as an independent test on the role of *Sox11* in the response of the retina to injury [1]. In this DBA/2J mouse model of pigment dispersion glaucoma, there were relatively low levels of *Sox11* in the control mice and in mice that did not have detectable levels of ganglion cell loss (Fig. 7). However, in mice with moderate ganglion cell loss, levels of *Sox11* were approximately four-fold higher than in control animals. In animals with severe glaucoma, the level of *Sox11* decreased to near control levels. These data suggest that the levels of *Sox11* decrease as the ganglion cells die. This transient upregulation of *Sox11* in moderate cases demonstrates the exquisite ability of *Sox11* to mark injured,

potentially dying neurons. As such, our data indicate that *Sox11* is a novel marker for injured neurons, specifically retinal ganglion cells.

What is the potential role of SOX11 following injury to the axons of the retinal ganglion cell? One hint comes from studies on the response of dorsal root ganglion neurons to peripheral nerve injury. *Sox11* is dramatically upregulated in the dorsal root ganglion following injury to the peripheral nerve and plays a pivotal role in axonal regeneration [9]. Three days after the transection of the sciatic nerve in the rat, there is a 1004% increase in *Sox11* in the dorsal root ganglion and these levels remain elevated for at least the next 4 days [9]. By 4 weeks after transection, *Sox11* levels have returned to baseline. This upregulation and sustained expression of *Sox11* is critical to the survival of the dorsal root ganglion neurons and the regeneration of peripheral axons along the injured nerve. When the levels of *Sox11* were knocked down by delivery of siRNA, there was an increase in apoptosis in cultured neurons as well as a decrease in neurite outgrowth in culture [23]. A similar decrease in axonal regeneration occured *in vivo* after *Sox11* knockdown in the dorsal root ganglion [9]. Thus, the upregulation of *Sox11* appears to be necessary for the normal regeneration of axons in the peripheral nerve. Interestingly, *Sox11* was also upregulated when the central projection of the dorsal root was severed; however, the degree of upregulation was lower, only 51% [9, 23]. Just like the neurons in the retina, the dorsal root ganglia did not regenerate their central projections into the adjacent spinal cord [35, 36]. This begs the question, why is *Sox11* upregulated in neurons of the retina and the dorsal root ganglion, when the axons will not successfully regenerate? The most parsimonious explanation is that these neurons are attempting to survive using the same program that is successful in peripheral nerve injury; however, other influences derail the regenerative program causing the cell to abort the regenerative process and, in many cases, cause subsequent neuronal death [37-40]. Recent evidence indicates that these inhibitory influences can at least be partially averted by stimulating the ganglion cells to regrow their axons [41-47]. Given that

upregulation of *Sox11* is among the initial responses of the neuron to injury and that this response is intact in retinal ganglion cells, it may be possible to identify where the transcriptional cascade leading to axon regeneration and cell survival in the CNS differs from that in peripheral nerve injury.

Acknowlegements

This work is supported by DoD Grant W81XWH1210255 from the U.S. Army Medical Research & Materiel Command and the Telemedicine and Advanced Technology (to EEG), NIH Grant R01EY017841 (to EEG), Vision Core Grant P030EY006360 (to P Michael Iuvone), and Unrestricted Funds from Research to Prevent Blindness (to Emory University).

References

1. Howell GR, Macalinao DG, Sousa GL, Walden M, Soto I, Kneeland SC, Barbay JM, King BL, Marchant JK, Hibbs M, Stevens B, Barres BA, Clark AF, Libby RT, John SW. Molecular clustering identifies complement and endothelin induction as early events in a mouse model of glaucoma. J Clin Invest 2011; 121(4):1429-44.
2. Moore DL, Goldberg JL. Multiple transcription factor families regulate axon growth and regeneration. Dev Neurobiol 2011; 71(12):1186-211.
3. Munguba GC, Geisert EE, Williams RW, Tapia ML, Lam DK, Bhattacharya SK, Lee RK. Effects of glaucoma on Chrna6 expression in the retina. Curr Eye Res 2013; 38(1):150-7.
4. Templeton JP, Freeman NE, Nickerson JM, Jablonski MM, Rex TS, Williams RW, Geisert EE. Innate immune network in the retina activated by optic nerve crush. Invest Ophthalmol Vis Sci 2013; 54(4):2599-606.
5. Vazquez-Chona FR, Geisert EE. Networks modulating the retinal response to injury: insights from microarrays, expression genetics, and bioinformatics. Adv Exp Med Biol 2012; 723:649-56.
6. Carlstedt T. Nerve fibre regeneration across the peripheral-central transitional zone. J Anat 1997; 190 (Pt 1):51-6.
7. Ramón y Cajal S, May RM. Degeneration & regeneration of the nervous system. London,: Oxford university press, Humphrey Milford; 1928.
8. McCurley AT, Callard GV. Time Course Analysis of Gene Expression Patterns in Zebrafish Eye During Optic Nerve Regeneration. J Exp Neurosci 2010; 2010(4):17-33.
9. Jankowski MP, McIlwrath SL, Jing X, Cornuet PK, Salerno KM, Koerber HR, Albers KM. Sox11 transcription factor modulates peripheral nerve regeneration in adult mice. Brain Res 2009; 1256:43-54.
10. Jing X, Wang T, Huang S, Glorioso JC, Albers KM. The transcription factor Sox11 promotes nerve regeneration through activation of the regeneration-associated gene Sprr1a. Exp Neurol 2012; 233(1):221-32.
11. Schepers GE, Teasdale RD, Koopman P. Twenty pairs of sox: extent, homology, and nomenclature of the mouse and human sox transcription factor gene families. Dev Cell 2002; 3(2):167-70.
12. Pillai-Kastoori L, Wen W, Morris AC. Keeping an eye on SOXC proteins. Dev Dyn 2015; 244(3):367-76.
13. Jiang Y, Ding Q, Xie X, Libby R, Lefebvre V, Gan L. Transcription factors SOX4 and SOX11 function redundantly to regulate the development of mouse retinal ganglion cells. J Biol Chem 2013.

14. Usui A, Iwagawa T, Mochizuki Y, Iida A, Wegner M, Murakami A, Watanabe S. Expression of Sox4 and Sox11 is regulated by multiple mechanisms during retinal development. FEBS Lett 2013; 587(4):358-63.
15. Wang Y, Lin L, Lai H, Parada LF, Lei L. Transcription factor Sox11 is essential for both embryonic and adult neurogenesis. Dev Dyn 2013; 242(6):638-53.
16. Haslinger A, Schwarz TJ, Covic M, Lie DC. Expression of Sox11 in adult neurogenic niches suggests a stage-specific role in adult neurogenesis. Eur J Neurosci 2009; 29(11):2103-14.
17. Usui A, Mochizuki Y, Iida A, Miyauchi E, Satoh S, Sock E, Nakauchi H, Aburatani H, Murakami A, Wegner M, Watanabe S. The early retinal progenitor-expressed gene Sox11 regulates the timing of the differentiation of retinal cells. Development 2013; 140(4):740-50.
18. Pillai-Kastoori L, Wen W, Wilson SG, Strachan E, Lo-Castro A, Fichera M, Musumeci SA, Lehmann OJ, Morris AC. Sox11 is required to maintain proper levels of Hedgehog signaling during vertebrate ocular morphogenesis. PLoS Genet 2014; 10(7):e1004491.
19. Wen W, Pillai-Kastoori L, Wilson SG, Morris AC. Sox4 regulates choroid fissure closure by limiting Hedgehog signaling during ocular morphogenesis. Dev Biol 2015; 399(1):139-53.
20. Bergsland M, Werme M, Malewicz M, Perlmann T, Muhr J. The establishment of neuronal properties is controlled by Sox4 and Sox11. Genes Dev 2006; 20(24):3475-86.
21. Tanaka S, Kamachi Y, Tanouchi A, Hamada H, Jing N, Kondoh H. Interplay of SOX and POU factors in regulation of the Nestin gene in neural primordial cells. Mol Cell Biol 2004; 24(20):8834-46.
22. Tanabe K, Bonilla I, Winkles JA, Strittmatter SM. Fibroblast growth factor-inducible-14 is induced in axotomized neurons and promotes neurite outgrowth. J Neurosci 2003; 23(29):9675-86.
23. Jankowski MP, Cornuet PK, McIlwrath S, Koerber HR, Albers KM. SRY-box containing gene 11 (Sox11) transcription factor is required for neuron survival and neurite growth. Neuroscience 2006; 143(2):501-14.
24. Templeton JP, Geisert EE. A practical approach to optic nerve crush in the mouse. Mol Vis 2012; 18:2147-52.
25. Hines-Beard J, Marchetta J, Gordon S, Chaum E, Geisert EE, Rex TS. A mouse model of ocular blast injury that induces closed globe anterior and posterior pole damage. Exp Eye Res 2012; 99:63-70.
26. Geisert EE, Jr., Frankfurter A. The neuronal response to injury as visualized by immunostaining of class III beta-tubulin in the rat. Neurosci Lett 1989; 102(2-3):137-41.
27. Schindelin J, Arganda-Carreras I, Frise E, Kaynig V, Longair M, Pietzsch T, Preibisch S, Rueden C, Saalfeld S, Schmid B, Tinevez JY, White DJ, Hartenstein V, Eliceiri K, Tomancak P, Cardona A. Fiji: an open-source platform for biological-image analysis. Nat Methods 2012; 9(7):676-82.
28. Freeman NE, Templeton JP, Orr WE, Lu L, Williams RW, Geisert EE. Genetic networks in the mouse retina: growth associated protein 43 and phosphatase tensin homolog network. Mol Vis 2011; 17:1355-72.
29. Barnstable CJ, Drager UC. Thy-1 antigen: a ganglion cell specific marker in rodent retina. Neuroscience 1984; 11(4):847-55.
30. Gan L, Xiang M, Zhou L, Wagner DS, Klein WH, Nathans J. POU domain factor Brn-3b is required for the development of a large set of retinal ganglion cells. Proc Natl Acad Sci U S A 1996; 93(9):3920-5.
31. Mu X, Beremand PD, Zhao S, Pershad R, Sun H, Scarpa A, Liang S, Thomas TL, Klein WH. Discrete gene sets depend on POU domain transcription factor

Brn3b/Brn-3.2/POU4f2 for their expression in the mouse embryonic retina. Development 2004; 131(6):1197-210.
32. Prasov L, Glaser T. Dynamic expression of ganglion cell markers in retinal progenitors during the terminal cell cycle. Mol Cell Neurosci 2012; 50(2):160-8.
33. Surgucheva I, Weisman AD, Goldberg JL, Shnyra A, Surguchov A. Gamma-synuclein as a marker of retinal ganglion cells. Mol Vis 2008; 14:1540-8.
34. Geisert EE, Lu L, Freeman-Anderson NE, Templeton JP, Nassr M, Wang X, Gu W, Jiao Y, Williams RW. Gene expression in the mouse eye: an online resource for genetics using 103 strains of mice. Mol Vis 2009; 15:1730-63.
35. Carlstedt T. Regrowth of anastomosed ventral root nerve fibers in the dorsal root of rats. Brain Res 1983; 272(1):162-5.
36. Liuzzi FJ, Lasek RJ. Astrocytes block axonal regeneration in mammals by activating the physiological stop pathway. Science 1987; 237(4815):642-5.
37. Geisert EE, Jr., Bidanset DJ, Del Mar N, Robson JA. Up-regulation of a keratan sulfate proteoglycan following cortical injury in neonatal rats. Int J Dev Neurosci 1996; 14(3):257-67.
38. Harel NY, Strittmatter SM. Can regenerating axons recapitulate developmental guidance during recovery from spinal cord injury? Nat Rev Neurosci 2006; 7(8):603-16.
39. Schwab ME, Bartholdi D. Degeneration and regeneration of axons in the lesioned spinal cord. Physiol Rev 1996; 76(2):319-70.
40. Silver J, Miller JH. Regeneration beyond the glial scar. Nat Rev Neurosci 2004; 5(2):146-56.
41. de Lima S, Koriyama Y, Kurimoto T, Oliveira JT, Yin Y, Li Y, Gilbert HY, Fagiolini M, Martinez AM, Benowitz L. Full-length axon regeneration in the adult mouse optic nerve and partial recovery of simple visual behaviors. Proc Natl Acad Sci U S A 2012; 109(23):9149-54.
42. Leibinger M, Muller A, Andreadaki A, Hauk TG, Kirsch M, Fischer D. Neuroprotective and axon growth-promoting effects following inflammatory stimulation on mature retinal ganglion cells in mice depend on ciliary neurotrophic factor and leukemia inhibitory factor. J Neurosci 2009; 29(45):14334-41.
43. Muller A, Hauk TG, Leibinger M, Marienfeld R, Fischer D. Exogenous CNTF stimulates axon regeneration of retinal ganglion cells partially via endogenous CNTF. Mol Cell Neurosci 2009; 41(2):233-46.
44. Park KK, Hu Y, Muhling J, Pollett MA, Dallimore EJ, Turnley AM, Cui Q, Harvey AR. Cytokine-induced SOCS expression is inhibited by cAMP analogue: impact on regeneration in injured retina. Mol Cell Neurosci 2009; 41(3):313-24.
45. Park KK, Liu K, Hu Y, Kanter JL, He Z. PTEN/mTOR and axon regeneration. Exp Neurol 2010; 223(1):45-50.
46. Pernet V, Joly S, Jordi N, Dalkara D, Guzik-Kornacka A, Flannery JG, Schwab ME. Misguidance and modulation of axonal regeneration by Stat3 and Rho/ROCK signaling in the transparent optic nerve. Cell Death Dis 2013; 4:e734.
47. Smith PD, Sun F, Park KK, Cai B, Wang C, Kuwako K, Martinez-Carrasco I, Connolly L, He Z. SOCS3 deletion promotes optic nerve regeneration in vivo. Neuron 2009; 64(5):617-23.

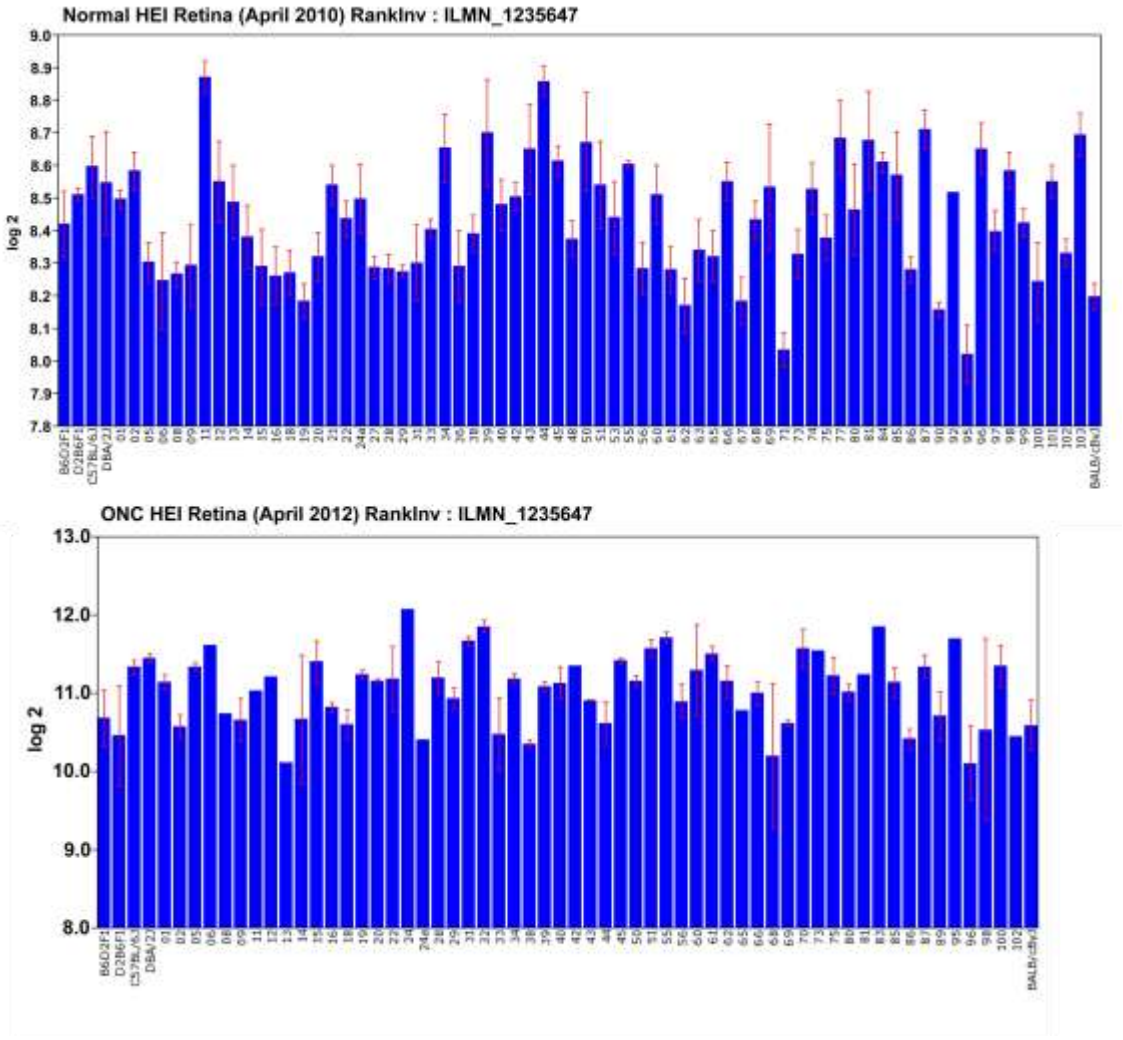

Figure 1. ***Sox11 Expression in the Normal Retina and After Optic Nerve Crush.*** The ordinate represents mRNA levels from microarrays, expressed in a $\log_2$ scale with the mean set to 8. The mice used to generate these data were C57BL/6J, DBA/2J, their respective F1 crosses, BALB/cByJ, and members of the BXD recombinant inbred strain line. The top graph denotes the expression levels of *Sox11* under normal conditions, while the bottom graph denotes the expression of *Sox11* two days after the optic nerve crush. Note the dramatic increase in expression following injury, from a normal mean expression value of 8.4 to a mean expression value of 11.0 after nerve crush.

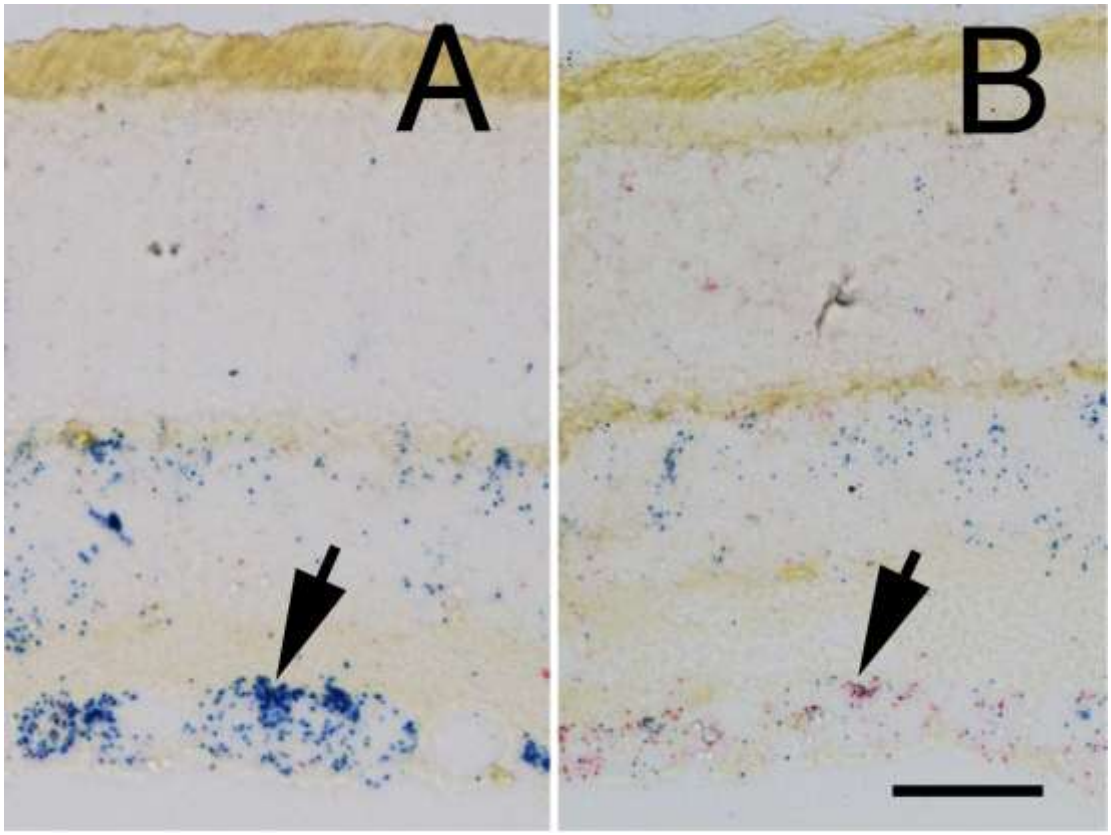

Figure 2. ***In Situ Hybridization for Sox11 and Chrna6.*** The distribution of *Sox11* and *Chrna6* mRNA was defined using two-color in situ hybridization for a section of control retina (A) and a section of a retina 2 days after optic nerve crush (B). The probe for *Chrna6* is shown in blue and that for *Sox11* in red. Note the extensive staining for *Chrna6* within the ganglion cell layer in the control section (Arrow in A). Two days after optic nerve crush there is already a substantial decrease in *Chrna6* expression. Very low levels of *Sox11* are seen in the control retina. There is a dramatic increase in *Sox11* staining after nerve crush within the retinal ganglion cells (Arrow in B). A and B are taken at the same magnification and the scale bar in B = 25 μm.

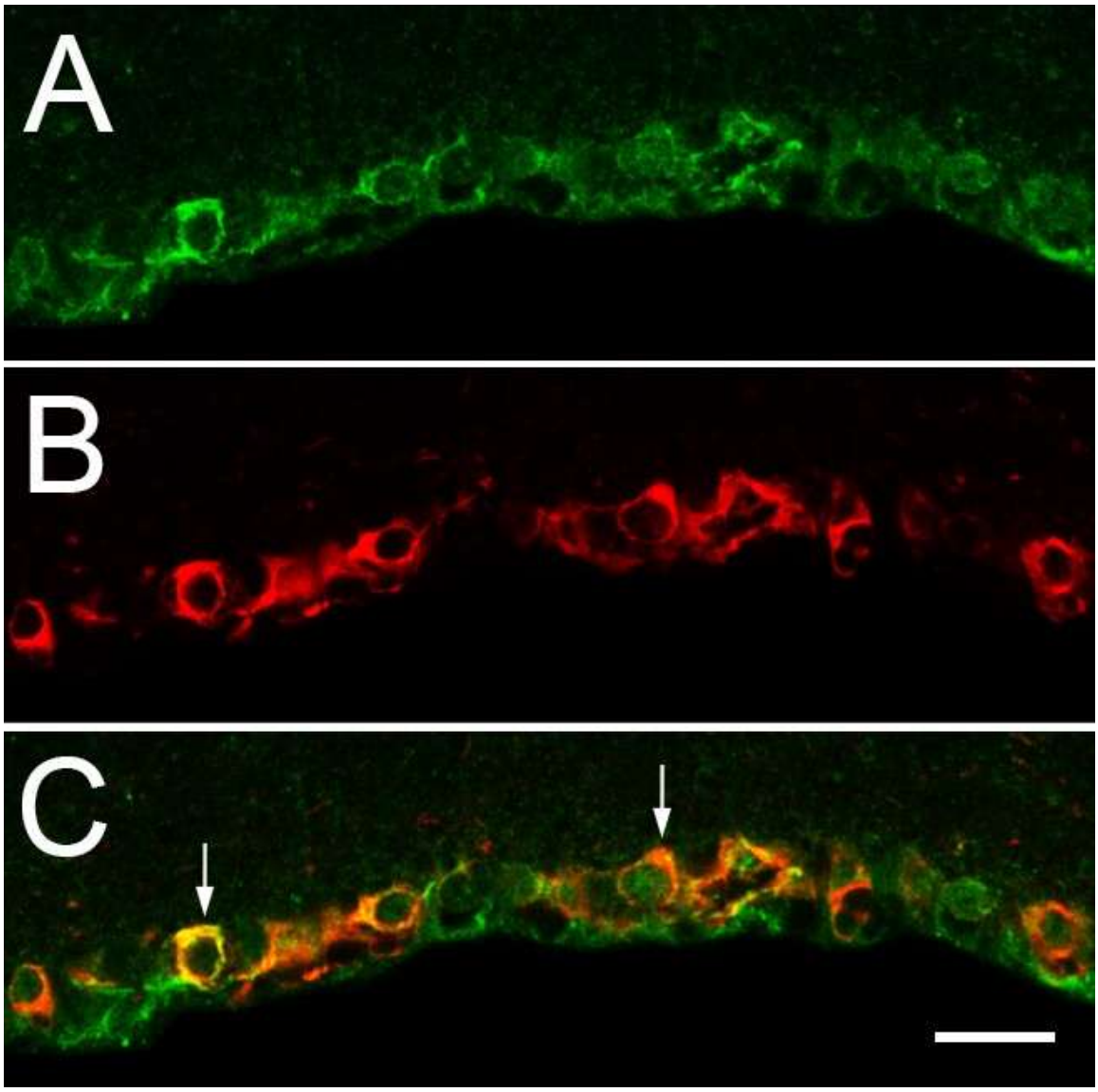

Figure 3. ***SOX11 Expression in Retinal Ganglion Cells.*** A section of retina, two days after optic nerve crush, was double stained for SOX11 (A) and class III beta tubulin (B), using double label indirect immunohistochemistry. Class III beta tubulin is a marker for retinal ganglion cells. In the merged image (C), retinal ganglion cells are double labeled (arrowhead) with SOX11 and Class III beta tubulin. Scale bar in C = 20 µm.

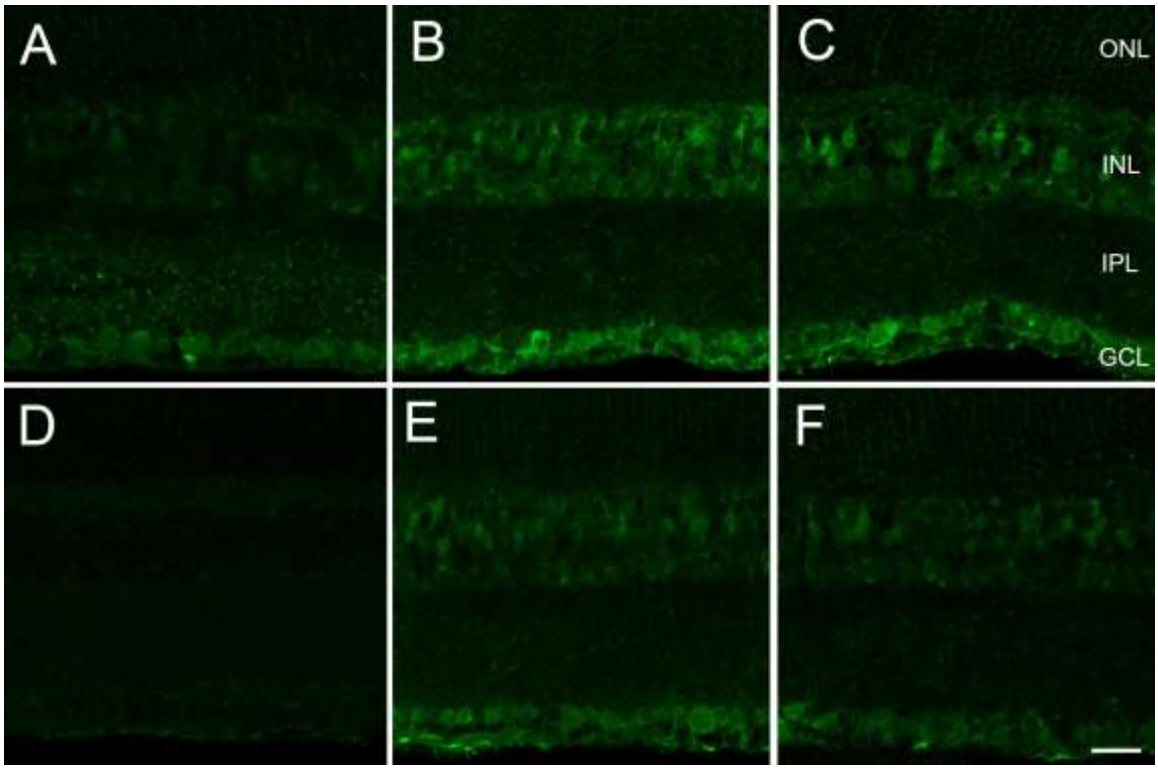

Figure 4. ***Upregulation of SOX11 After Retinal Injury.***

Retinal sections were stained with an antibody directed against SOX11 in the following conditions: normal retina (A), retina two (B) and five (C) days after optic nerve crush, and retina two (E) and five (F) days after blast injury. The negative control without primary antibody is shown in (D). After injury to the retina, there is a dramatic increase in the intensity of staining within the cell bodies of retinal ganglion cells, and some cells in the INL. The layers of the retina are labeled: ONL (outer nuclear layer), INL (inner nuclear layer) and GCL (ganglion cell layer). All photomicrographs are presented at the same magnification and the scale bar in F = 20 µm.

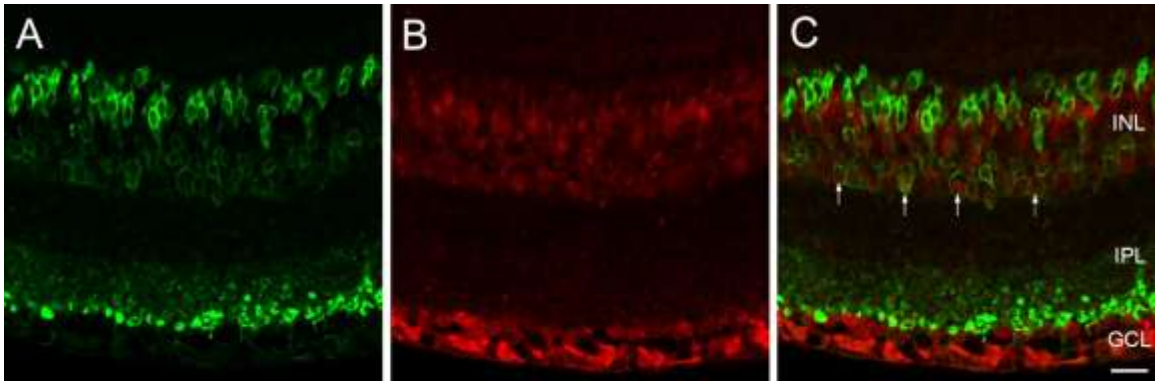

Figure 5. Upregulation of SOX11 in the Inner Nuclear Layer Following Injury.

Retinas were stained with antibodies directed against PKC alpha to label bipolar cells (A) and Sox11 (B) two days after optic nerve crush. In the merged image (C), about half of the bipolar cells are double-labeled, and they are mostly localized to the inner part of the INL (arrowheads).

The layers of the retina are labeled: ONL (outer nuclear layer), INL (inner nuclear layer) and GCL (ganglion cell layer). All photomicrographs are presented at the same magnification and the scale bar in C = 20 μm.

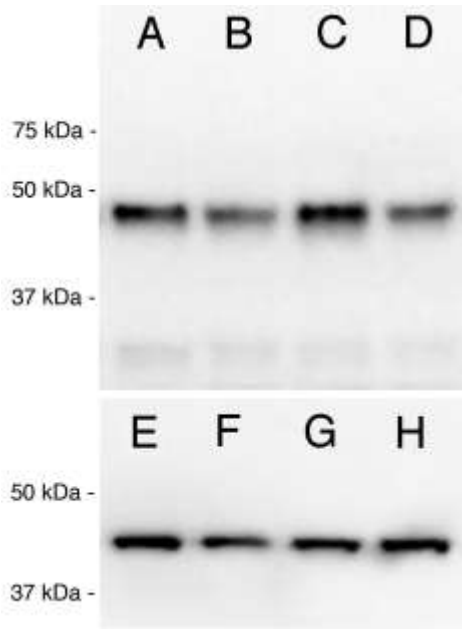

Figure 6. ***Upregulation of SOX11 protein after optic nerve crush*****.** Immunoblots of protein samples from normal retina (B and D) and from retinas 2 days after optic nerve crush (A and C) were probed with antibodies directed against SOX11. There was increased staining of the bands from the optic nerve crush samples relative to the normal retinal samples. Loading control in E-H: beta-actin.

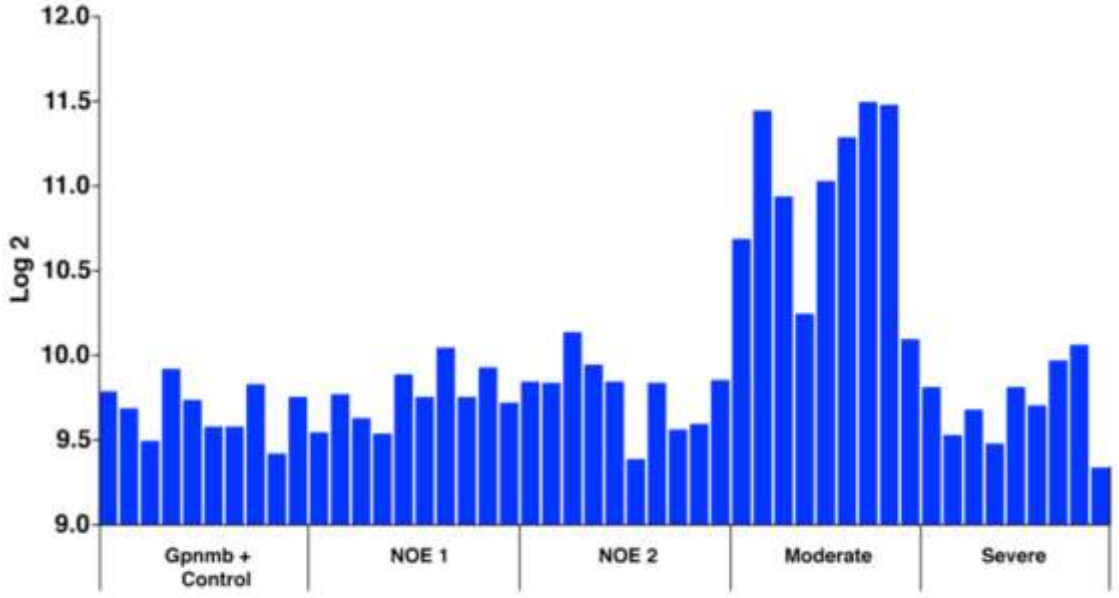

Figure 7. ***Sox11 mRNA Levels in Pigmentary Glaucoma***. *Sox11* levels in a meta-analysis of a DBA/2J mouse pigmentary glaucoma dataset from Howell et al. (2011). The ordinate represents the *Sox11* mRNA level from microarrays, expressed in $\log_2$, scaled with the mean set to 8. The mice were classified as wild type *Gpnmb*$^{+/+}$ controls (Gpnmb+ Controls), no detectable glaucoma 1 (NOE 1), no detectable glaucoma 2 (NOE2), moderate glaucoma (Moderate), and severe glaucoma (Severe). Other than the wild type group, all the groups were *Gpnmb*$^{-/-}$. Notice that there is a dramatic increase in *Sox11* expression during early phases of glaucoma in this mouse model. As the ganglion cells die in severe glaucoma, the expression levels of *Sox11* appear to decrease. These data suggest that *Sox11* is an early marker for retinal injury. This general expression pattern was observed for the following 5 of the 6 Affymetrix probe sets targeting *Sox11*: 1429051_s_at (illustrated above), 1453002_at, 1429372_at, 1453125_at and 1431225_at.